

## Comparison of Ozone Formation Attribution Techniques in the Northeast United States

### Source Attribution of Ozone and Precursors in the Northeast U.S. Using Multiple Photochemical Model Based Approaches (CMAQ v5.3.2 and CAMx v7.10)

Qian Shu<sup>1</sup>, Sergey L. Napelenok<sup>1</sup>, William T. Hutzell<sup>1</sup>, Kirk R. Baker<sup>1</sup>, Benjamin Murphy<sup>1</sup>, Christian Hogrefe<sup>1</sup>, Barron H. Henderson<sup>1</sup>

<sup>1</sup>U.S. Environmental Protection Agency, Research Triangle Park, NC, 27711, USA.

Correspondence to: Sergey L Napelenok ([sergey.napelenok@epa.gov](mailto:sergey.napelenok@epa.gov))([sergey.napelenok@epa.gov](mailto:sergey.napelenok@epa.gov))

#### 10 **Abstract.**

The Integrated Source Apportionment Method (ISAM) has been revised in the Community Multiscale Air Quality (CMAQ) model. This work updates ISAM to maximize its flexibility, particularly for ozone (O<sub>3</sub>) modeling, by providing multiple attribution options, including products inheriting attribution fully from nitrogen oxide reactants, fully from volatile organic compound (VOC) reactants, equally to all reactants, or dynamically to NO<sub>x</sub> or VOC reactants based on the indicator gross production ratio of hydrogen peroxide (H<sub>2</sub>O<sub>2</sub>) to nitric acid (HNO<sub>3</sub>). The updated ISAM has been incorporated into the most recent publicly accessible versions of CMAQ (v5.3.2 and beyond). This study's primary objective is to document these ISAM updates and demonstrate their impacts on source apportionment results for O<sub>3</sub> and its precursors. Additionally, the ISAM results are compared with the Ozone Source Apportionment Technology (OSAT) in the Comprehensive Air-quality Model with Extensions (CAMx) and the brute force method (BF). All comparisons are performed for a 4km horizontal grid resolution application over the northeast U.S. for a selected two-day summer case study (August 9th and 10th, 2018). General similarities among ISAM, OSAT, and BF results add credibility to the new ISAM algorithms. However, some discrepancies in magnitude or relative proportions among tracked sources illustrate the distinct features of each approach while others may be related to differences in model formulation of chemical and physical processes. Despite these differences, OSAT and ISAM still

provide useful apportionment data by identifying the geographical and temporal contributions of O<sub>3</sub> and its precursors. Both OSAT and ISAM attribute the majority of O<sub>3</sub> and NO<sub>x</sub> contributions to boundary, mobile, and biogenic sources, whereas the top three contributors to VOCs are found to be biogenic, boundary, and area sources.

## 1 Introduction

Tropospheric O<sub>3</sub> is a critical air pollutant that endangers human health (WHO, 2013) and sensitive vegetation (Booker et al., 2009), and contributes to climate change (Jacob and Winner, 2009). It is produced through non-linear photochemical reactions of carbon monoxide (CO), volatile organic compounds (VOC), and nitrogen oxides (NO<sub>x</sub> = NO + NO<sub>2</sub>) with sunlight (Atkinson, 2000). In the United States, the national average ambient O<sub>3</sub> concentration has decreased by 22% since 1990, owing to regulations such as the Clean Air Act (CAA) on NO<sub>x</sub> and VOC emissions (Simon et al., 2015). Long-term space observations have also confirmed the improvement in air quality (Duncan et al., 2013; Lamsal et al., 2015). However, many major metropolitan areas continue to exceed the O<sub>3</sub> national ambient air quality standards (NAAQS) set by the US Environmental Protection Agency (US EPA). To continue to reduce O<sub>3</sub> levels, it is critical to develop effective emission control strategies as has been done for other pollutants (Lefohn et al., 1998; Reitze, 2004; Cooper et al., 2015). The effectiveness of any O<sub>3</sub> control strategy hinges on accurately quantifying the contributions of various precursor emissions to O<sub>3</sub> formation.

Numerous techniques have been used to characterize and quantify the relationship between emission sources and ~~ozone~~O<sub>3</sub> concentrations, including statistical methods, model sensitivity simulations, and model source apportionment approaches, each with its own set of advantages and disadvantages (Cohan and Napelenok, 2011). While some traditional receptor-based methods based on chemical mass balance (CMB, Hidy and Friedlander, 1971), such as Effective Variance solution (EV, Watson et al., 1984) and Positive Matrix Factorization (PMF, Paatero and Tapper, 1994), produce insightful results when measurements are taken at a specific receptor, they are typically applied to speciated VOC and particulate matter (PM) and are also constrained by the relative sparsity of observations in space and time, rendering them unsuitable for regional and national O<sub>3</sub> precursor

emission control strategies. Alternatively, three-dimensional air quality models (AQM) allow for the  
55 quantification of O<sub>3</sub> source contributions at regular intervals over longer periods and wider spatial  
distributions. The most basic source apportionment (SA) technique in the context of an AQM is to  
conduct source sensitivity simulations using the brute force (BF) method, in which several simulations  
are conducted, each with one source eliminated or reduced. The differences in the output fields  
compared to the baseline simulation are then attributed to the eliminated or reduced source (e.g.,  
60 Marmur et al., 2005). BF has some limitations when used to determine total source culpability of O<sub>3</sub> due  
to the pollutants' nonlinear dependence on both relative and absolute VOC and NO<sub>x</sub> concentrations. For  
example, ~~at some chemical regimes where the ambient ratio of total VOC to total NO<sub>x</sub> concentrations is  
sufficiently low,~~ removing NO<sub>x</sub> may lead to an increase ~~in~~<sup>of</sup> O<sub>3</sub> concentrations, ~~because NO<sub>x</sub> also acts  
in the vicinity of large NO emissions (e.g., power plants), as a titrant~~<sup>the result of net conversion</sup> of O<sub>3</sub> to  
65 ~~NO<sub>2</sub> (Gillani et al., 1996) or at night-time when NO<sub>x</sub> titration cannot be balanced by the photolysis of  
NO<sub>2</sub>.~~ In some cases, where a source contributes a substantial portion of total NO<sub>x</sub> or VOC emissions,  
complete source removal for the purposes of source apportionment calculation may also substantially  
alter the underlying chemical regime for formation of secondary pollutants such as O<sub>3</sub>. Further, to  
separate the contributions and interactions of “n” sources, Stein and Alpert (1993) showed that BF  
70 would require two to the power of the number of sources (2<sup>n</sup>). This is quickly impractical leading to a  
subset of BF simulations with unknown interactions. As a result, summarizing the O<sub>3</sub> change in  
response to multiple brute force emission source simulations can make it difficult to interpret the  
cumulative effect of those emissions on O<sub>3</sub> (Kwok et al., 2015).

Reactive tracer or tagged species SA methods for O<sub>3</sub> have also been incorporated in AQMs.  
75 These tracers are usually additional species added to the AQM to track the contributions of pollutants  
from specific source categories. They undergo the same atmospheric processes as the bulk chemical  
species within the model (Kwok et al, 2015). As one example, OSAT within CAMx quantifies the  
contributions of various emission sectors, source regions, as well as initial and lateral boundary  
conditions, to simulated O<sub>3</sub> concentrations (Ramboll Environ, 2015). OSAT allocates instantaneous O<sub>3</sub>  
80 formation to either NO<sub>x</sub> or VOCs based on the ratio of hydrogen peroxide (H<sub>2</sub>O<sub>2</sub>) to nitric acid (HNO<sub>3</sub>)  
production (Dunker et al., 2002). O<sub>3</sub> formation is classified as being NO<sub>x</sub>-limited or VOC-limited based

Formatted: Subscript

on the gross production of H<sub>2</sub>O<sub>2</sub> (PH<sub>2</sub>O<sub>2</sub>) and HNO<sub>3</sub> (PHNO<sub>3</sub>). When the ratio (PH<sub>2</sub>O<sub>2</sub>/PHNO<sub>3</sub>) is ~~below~~<sup>above</sup> 0.35, the formation is classified as NO<sub>x</sub>-limited and VOC-limited otherwise (Sillman, ~~1996~~<sup>1995</sup>). If the photochemical formation of O<sub>3</sub> (PO<sub>3</sub>) occurs in a NO<sub>x</sub>-limited regime, the NO<sub>x</sub> tracers  
85 are used to attribute PO<sub>3</sub> proportionally to the emissions sources that contributed to the NO<sub>x</sub> concentrations. Otherwise, VOC tracers are used to attribute PO<sub>3</sub> to the sources that contributed to the VOC concentrations (Dunker et al., 2002; Kwok et al., 2015). The OSAT formulation was recently changed (OSAT3) to track all forms of NO<sub>x</sub> to account for NO<sub>x</sub> recycling, which occurs when NO<sub>x</sub> is converted to another form of NO<sub>x</sub> (e.g., peroxyacetyl nitrate (PAN) or HNO<sub>3</sub>) and then converted back  
90 to NO<sub>x</sub>. OSAT has been used to support policy assessments (e.g., U.S. EPA, state government agencies, etc., Ramboll Environ, 2015, 2022) as well as for scientific research purposes (Li et al., 2012; Zhang et al., 2017; Shu et al., 2020).

Additionally, the Integrated Source Apportionment Method (ISAM) within CMAQ has shown promising results for O<sub>3</sub> tagging (Kwok et al., ~~2013~~, 2015). Recent ISAM experiments have quantified  
95 the contribution of O<sub>3</sub> sources to air pollution in several major cities throughout the United States and Europe (Kwok et al., 2015; Valverde et al., ~~2016a~~<sup>2016</sup>; Karamchandani et al., 2017; Butler et al., 2018; Pay et al., 2019). The attribution of O<sub>3</sub> and precursors from specific sources estimated by ISAM implemented in version 5.0 of CMAQ compared well with source-specific aircraft transect measurements (Baker and ~~Kelly, 2014~~; ~~Baker and~~ Woody, ~~2017~~<sup>2016</sup>). The ISAM algorithms have also  
100 been updated several times following the original implementation in CMAQv5.0.2.

ISAM updates presented ~~herein this study~~ substantially increase the flexibility to the user of the CMAQ source apportionment model. ~~These updates were intended to provide long term flexibility within the model to accommodate newer chemical mechanisms, and are described in detail below. changed the attribution approach as detailed in the methods section. These flexibilities allow for~~  
105 ~~apportionment of more species and allow for more methods of apportionment.~~ Further in the manuscript we apply the changes to CMAQ-ISAM for a Northeastern U.S. O<sub>3</sub> air quality episode and compare the results to CMAQ-BF and CAMx-OSAT. The manuscript is organized as follows: Section 2 documents the ISAM updates in detail; Section 3 describes the methodology for this study, which includes the base modeling configurations, simulation designs for source apportionment, tracked species classes,

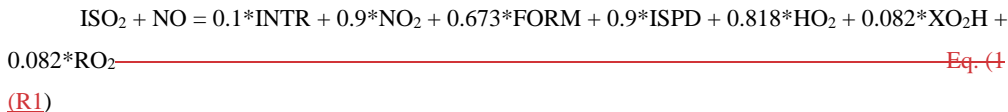
Formatted: English (United States)

110 evaluation methods, and case study development; Section 4 presents the findings, including model  
evaluation results and comparisons of source apportionment for several species; Section 5 documents  
the running speed comparisons between CMAQ-ISAM, CAMx-OSAT and CMAQ-BF; and finally, the  
findings and their implications for future research are discussed in Section 6.

## 2.2 Source apportionment methods

### 2.1 Updates in ISAM

115 The ISAM implementation in the version 5.0 release of CMAQ was based on Kwok et al. (2013)  
and Kwok et al. (2015). That approach was then updated ~~in~~ starting from CMAQ version 5.3 to an  
attribution based on integrated reaction rates and product yields (US EPA, 2021/2019). The ~~later~~  
~~versions (v5.3-version.2 and beyond)~~ of CMAQ-ISAM (US EPA, 2022) ~~employs~~ employ an  
120 apportionment scheme that assigns products of each chemical reaction to sources based on reactant  
stoichiometry ~~(US EPA, 2021)~~. For example, the isoprene peroxy radical (ISO<sub>2</sub>) reacts with nitric  
oxide (NO) to produce several different stable and radical species as represented in the CB6R3 chemical  
mechanism by the following ~~equation (Equation 1)~~ reaction R1.



In addition to nitrogen dioxide (NO<sub>2</sub>), the products include isoprene nitrate (INTR),  
formaldehyde (FORM), hydroperoxy ~~radical~~radicals (HO<sub>2</sub>), alkoxy radicals (XO<sub>2</sub>H), peroxy  
~~radical~~radicals (RO<sub>2</sub>), and other isoprene reaction products (ISPD). -ISO<sub>2</sub> ~~itself~~ is a ~~direct~~ product  
130 ~~from of the~~ oxidation of isoprene ~~in the chemical mechanism~~, which, ~~in turn~~, originates from  
overwhelmingly biogenic sources. ~~Conversely~~, NO is typically emitted from anthropogenic combustion  
processes, with a much smaller natural component originating from lightning strikes and microbial soil  
processes ~~on the global scale~~ (Jacquemin et al., 1990; Yienger et al., 1995; ~~Pierce et al., 1999~~) ~~on the~~  
~~global scale~~). Thus, the reactants ~~of this reaction~~ are approximately half from biogenic and half from  
135 anthropogenic sources ~~resulting in, so~~ the ~~reaction's~~ products ~~listed above inheriting~~ have the same

Formatted: Heading 3

Formatted: Indent: First line: 0.5"

attribution distribution. However, source attribution approaches, both receptor-based (such as PMF) and source-based (such as ISAM), are often used to understand how originally emitted NO<sub>x</sub> and VOC from particular sources ultimately contribute to model-predicted O<sub>3</sub> production. Therefore, the loss of source identity through processes, such as the photo-stationary state (PSS) null-NO<sub>x</sub> cycle (Leighton, 1961) or enhancing the influence and the role of organic peroxy radicals from sources that are not controlling O<sub>3</sub> production due to nonlinear chemistry, could shift-determine the culpability of emission sources. In the preceding example, the NO<sub>2</sub> produced by Equation 1 inherits the R1 is assigned a source that is approximately 50% biogenic and 50% anthropogenic. These types of source assignments can propagate quickly in situations where the PSS causes when catalytic processes cause NO<sub>2</sub> to cycle back to NO through photooxidation and radical oxidation with increasingly higher attribution to biogenic sources. Since NO<sub>x</sub> cycling is a fast process in the context of regional air pollution modeling models, anthropogenically emitted nitrogen species can become assigned to biogenic (or other nearby) sources downwind because, so the original emitted-source identity was not retained through these complex reactions. Equation 1, R1 is just one example that illustrates the complex relationship between precursors and subsequent source identities of secondary pollutants. Many such reactions exist in modern chemical mechanisms, which themselves are a simplification of the actual atmosphere. In some source apportionment applications, such as in the context of O<sub>3</sub> source attribution assessments, nitrogen focus on how sources induce O<sub>3</sub> production above background levels. Nitrogen molecules should then retain their original source signatures. This is also the approach is used by other apportionment models such as OSAT, earlier ISAM implementations (Kwok et al., 2015), and other tagging methods such as those developed by (Butler et al., 2018) and Grewe et al., 2010).

Since attribution objectives may vary based on scale (e.g., global compared to urban) or purpose (e.g., policy or tracing chemical reactions), ISAM has been enhanced to provide additional configuration options for the user to define how secondarily formed gaseous species are assigned to sources of parent reactants (Table 1) (US EPA 2022-2022b). The original-assignment existing scheme with equal source assignment based on reaction stoichiometry stoichiometrically proportional product attribution introduced in CMAQ version 5.3.2 (US EPA 2021) was has been retained as ISAM-OP1.

Formatted: Default Paragraph Font, Font color: Auto, Border: : (No border)

Formatted: Default Paragraph Font, Font color: Auto, Border: : (No border)

Formatted: Not Superscript/ Subscript

option 1 (ISAM-OP2 was OP1). Four new options have been added to give the user the option to  
165 always assign products to sources emitting nitrogen reactants can configure their simulation based on  
the application's goal. Each option allows for greater retention of source identity based on subsets of  
species in the chemical mechanism. ISAM-OP2 apportions products according to the source identity of  
reactive nitrogen species, including NO, NO<sub>2</sub>, nitrate radical (NO<sub>3</sub>), nitrous acid (HONO), and/or  
HNO<sub>3</sub>, dinitrogen pentoxide (N<sub>2</sub>O<sub>5</sub>), and aerosol nitrate (ANO<sub>3</sub>). Sources without these species utilize  
170 an assignment approach consistent with ISAM-OP1. ISAM-OP3 was added to include the nitrogen  
species from ISAM-OP2 with the addition of all For example, CB6R3 contains the reactive VOCs and  
intermediary organic radicals participating in ozone chemistry as initial source assignment criteria,  
completing following reaction between the list of species important in O<sub>3</sub> chemistry. ISAM-OP4 was  
added to allow methyl peroxy radical (MEO<sub>2</sub>) and NO:



175 In the user to assign product to only sources with original ISAM-OP1 configuration, the reactive  
VOCs products of R2, FORM, HO<sub>2</sub>, and radicals if present, NO<sub>2</sub> inherit source identities proportional to  
the source identities of the reactants (MEO<sub>2</sub> and with an ISAM-OP1 assignment if not present, NO).  
However, ISAM-OP2 apportions the product to be from the source identity of NO (presumed  
180 predominantly anthropogenic), because NO is a weighted nitrogen-containing species. When a  
reaction's reactants do not include any of the weighted species, products are apportioned to source  
identities using the same methodology used in OP1.

ISAM-OP3 expands OP2's list of weighted species to include VOC species identified as  
important to O<sub>3</sub> production. In CB6R3, this includes aldehydes (ALD<sub>2</sub> and ALDX), FORM, acetone  
185 (ACET), lumped ketones (KET), peroxy operators (XO<sub>2</sub> and XO<sub>2</sub>H), ISO<sub>2</sub>, acetyl peroxy radicals (C<sub>2</sub>O<sub>3</sub>  
and CXO<sub>3</sub>). Therefore, products of reactions containing these VOCs in addition to the nitrogen species  
of OP2 as reactants would inherit these species' source identities. For example, ALD<sub>2</sub> reacts with the  
NO<sub>3</sub> as follows in CB6R3.



190 The reaction's products, C<sub>2</sub>O<sub>3</sub> and HNO<sub>3</sub>, inherit identities equally divided between the sources  
of the reactants because ALD<sub>2</sub> and NO<sub>3</sub> are on the list of OP3 species. Reactions without any of these

species in the reactants list, like OP2, have their products apportioned to source using OP1's methodology when the reactants are not among the weighted ones.

ISAM-OP4 lists only VOC species and daughter products instrumental in O<sub>3</sub> chemistry as defined in OP3. In the R1 example, the products are apportioned to the source identity of ISO<sub>2</sub>, because the other reactant, NO, is not on the list of weight species. Similarly, the products of R3 are attributed to the source identity of ALD<sub>2</sub>. As in options 2 and 3, reactions (such as R2) without any listed species are attributed as in OP1's method.

Finally, ISAM-OP5 was added to make the assignment decision based on the account for the instantaneously calculated O<sub>3</sub> formation regime or limiting case. The regime is determined using the ratio of PH<sub>2</sub>O<sub>2</sub> to PHNO<sub>3</sub>. The transition point between regimes has a default value equal to 0.35 (Sillman, 1996). Assignment is made to sources with NO<sub>x</sub> species (ISAM-OP2) or to VOC species (ISAM-OP4) considering whether the O<sub>3</sub>-producing chemical regime is 1995). For the NO<sub>x</sub>-limited regime (PH<sub>2</sub>O<sub>2</sub>/PHNO<sub>3</sub>>0.35), source identity is passed from the nitrogen species of OP2, while for the VOC-limited regime (PH<sub>2</sub>O<sub>2</sub>/PHNO<sub>3</sub>≤0.35 as the threshold), source identity is passed from the organics of OP4. These CMAQ-ISAM options, including the regime threshold value (or transition point), are accessible to users at runtime through the standard model run script.

Table 1. Expanded CMAQ-ISAM options.

CMAQ ISAM option	Description	Reaction product source identity assignment	Representative CB6R3* Species
ISAM-OP1	Source attribution uniformly based on stoichiometric reaction rate products. Proportional to stoichiometry of all reactants.		All tracked model species
ISAM-OP2	Assignment proportional to sources with NO, NO <sub>2</sub> , NO <sub>3</sub> , HONO, or ANO <sub>3</sub> if present in parent stoichiometry of nitrogen containing reactants, otherwise proportional assignments same as ISAM-OP1.		NO, NO <sub>2</sub> , NO <sub>3</sub> , HONO, HNO <sub>3</sub> , N <sub>2</sub> O <sub>5</sub> , ANO <sub>3</sub>
ISAM-OP3	Assignment proportional to sources with species from ISAM-OP2 in addition to stoichiometry of key O <sub>3</sub>		NO, NO <sub>2</sub> , NO <sub>3</sub> , HONO, HNO <sub>3</sub> , N <sub>2</sub> O <sub>5</sub> , ANO <sub>3</sub> , ALD <sub>2</sub> , ALDX, FORM,

Inserted Cells

Formatted Table



	chemistry reactants (reactive VOC species* and VOCs, radicals if present in parent reactants, nitrogen species), otherwise proportional assignments same as ISAM-OP1.	ACET, KET, XO <sub>2</sub> , XO <sub>2</sub> H, ISO <sub>2</sub> , C <sub>2</sub> O <sub>3</sub> , CXO <sub>3</sub>
ISAM-OP4	Assignment Proportional to sources with reactive stoichiometry of VOC species and radicals if present in parent radical containing reactants, otherwise proportional assignments same as ISAM-OP1.	ALD <sub>2</sub> , ALDX, FORM, ACET, KET, XO <sub>2</sub> , XO <sub>2</sub> H, ISO <sub>2</sub> , C <sub>2</sub> O <sub>3</sub> , CXO <sub>3</sub>
ISAM-OP5	Assignment based on According to the ratio of PH <sub>2</sub> O <sub>2</sub> to PHNO <sub>3</sub> for species in O <sub>3</sub> chemistry reactants present, otherwise same as ISAM-OP1.	NO <sub>x</sub> -limited: NO, NO <sub>2</sub> , NO <sub>3</sub> , HONO, HNO <sub>3</sub> , N <sub>2</sub> O <sub>5</sub> , ANO <sub>3</sub> VOC-limited: ALD <sub>2</sub> , ALDX, FORM, ACET, KET, XO <sub>2</sub> , XO <sub>2</sub> H, ISO <sub>2</sub> , C <sub>2</sub> O <sub>3</sub> , CXO <sub>3</sub>
VOC-NO <sub>x</sub> limiting Transition Point	Value of the above ratio where assignment changes from species groups (default 0.35).	

Formatted: Subscript

\*Species are based on CB6R3 and may vary based on different chemical mechanisms implemented in CMAQ. Details can be found in SA\_DEFN.F in the CMAQ source code.

Formatted: Font: 10 pt

## 2.2 OSAT description

The source apportionment approach implemented in CAMx is briefly recapped here. Detailed updates of all OSAT versions can be found in the CAMx official user guide ([https://camx.com/Files/CAMxUsersGuide\\_v7.10.pdf](https://camx.com/Files/CAMxUsersGuide_v7.10.pdf)). All available versions of OSAT (including OSAT3) in CAMx separately solve for production and destruction of O<sub>3</sub> with production being attributed to either NO<sub>x</sub> or VOC emissions, depending on which is estimated to be limiting O<sub>3</sub> production. When the ratio of PH<sub>2</sub>O<sub>2</sub>/PHNO<sub>3</sub> exceeds 0.35, the produced O<sub>3</sub> is attributed to NO<sub>x</sub> emissions, and VOC emissions below that threshold. The CAMx source apportionment implementation includes an option (OSAT-APCA) that allows for a redirection of attribution to anthropogenic emissions in situations where the limiting precursor is biogenic. In CAMx-OSAT, O<sub>3</sub> attributed to NO<sub>x</sub> and VOCs is tracked as separate tracer groups. O<sub>3</sub> tracers are first adjusted to account for O<sub>3</sub> destruction processes and subsequently for net O<sub>3</sub> production, which is defined as the difference between O<sub>3</sub> production and O<sub>3</sub> destruction based on a subset of photochemical reactions that result in O<sub>3</sub>

Formatted: Not Superscript/ Subscript

Formatted: 006 Body Text

230 destruction. In situations where the net O<sub>3</sub> production is negative (destruction reactions dominate), all the O<sub>3</sub> tracers are proportionally decreased. When net O<sub>3</sub> production is positive, production is <sup>species</sup> assigned proportionally to the sources for each option are listed in Table S3 of those emissions (NO<sub>x</sub> and VOC precursor tracers) at the time and place where O<sub>3</sub> was made. OSAT includes a group of tracers that track odd-oxygen that is consumed when O<sub>3</sub> reacts with NO to form NO<sub>2</sub> that can quickly photolyze and reform O<sub>3</sub> through a reaction with oxygen. In this situation, the O<sub>3</sub> removed from the O<sub>3</sub> tracers due to the NO + O<sub>3</sub> reaction is moved to the odd-oxygen tracers (which have separate NO<sub>x</sub> and VOC tracer groups). When NO<sub>2</sub> is photolyzed and O<sub>3</sub> formed a proportional amount of O<sub>3</sub> is taken from the odd-oxygen tracers and moved to the O<sub>3</sub> tracers.

Formatted: Not Superscript/ Subscript

Formatted: Not Superscript/ Subscript

Formatted: Not Superscript/ Subscript

Formatted: Not Superscript/ Subscript

## 235 **3 Method**

### **3.1 Base model configurations**

Two models, CMAQ version 5.3.2 with modified ISAM and CAMx version 7.10 with OSAT3, are used to simulate a one-month period during the summer of 2018 (July 29<sup>th</sup> to August 30<sup>st</sup>). The summary of the two model configurations is presented in Table 2. Both models are applied to the same horizontal modeling domain with 4 km x 4 km resolution encompassing the northeastern United States. This domain is nested within a larger 12 km domain that encompasses the entire contiguous United States which is used for providing simulation boundary and initial conditions (BC and IC) for the 4 km domain. BCs were generated for the 12 km simulations using a hemispheric application of the GEOS-Chem model (Henderson et al., 2014) that was run for 2018. Anthropogenic emissions were based on version 1 of the 2016 National Emission Inventory (NEI, US EPA, 2021). Electrical Generating Unit emissions were based on continuous emissions monitoring data from 2018 where available. Onroad emissions were projected to 2018 to reflect decreases in emissions due to vehicle fleet turnover and the implementation of emission control technology in 2017. The Biogenic Emission Inventory System (Bash et al., 2016) was used to generate biogenic volatile organic compound emissions, and offline meteorology was created using the Weather Research and Forecasting (WRF, Skamarock et al., 2008) model version 3.8. CMAQ was configured using Carbon Bond 6 version 3 (CB6R3, Emery et al., 2015)

240

245

250

for chemistry. Similarly, all base meteorological and emissions inputs for CAMx were identical to those for CMAQ but were processed using CAMx appropriate data pre-processors (<https://www.camx.com>). The CAMx model was configured with Carbon Bond 6 version 4 (CB6R4, Emery et al., ~~2016~~ [2016a](#)) ~~chemical mechanism. Table 1 contains the summary of the two model configurations.~~ [2016a](#)) ~~chemical mechanism. It is noteworthy that the major updates for CB6R4 from CB6R3 are to (1) replace full marine halogen chemistry with a condensed iodine mechanism called "I-16," which could reduce O<sub>3</sub> depletion over marine areas, and (2) add dimethyl sulfide (DMS) chemistry. Emery et al. (2016b) demonstrated that the difference in O<sub>3</sub> decrements between full halogen chemistry and I-16 is small and can be neglected over land.~~

**Table 2. CMAQ and CAMx model configurations**

Model option	CMAQ	CAMx
Model version	Version 5.3.2	Version 7.10
Horizontal resolution	4 km	4 km
Vertical layers	35	35
Meteorology	WRF3.8	WRF3.8
Anthropogenic Emissions	2016 NEI version 1 <sup>a</sup>	2016 NEI version 1 <sup>b</sup>
Biogenic Emissions	BEIS <sup>c</sup>	BEIS <sup>c</sup>
BC/IC	12km US CONUS	12km US CONUS
Gas phase chemistry	CB6R3	CB6R4
Source apportionment	ISAM	OSAT3

<sup>a</sup>EGU were based on continuous emissions monitoring data from 2018 where available. Onroad emissions were projected to 2018.

<sup>b</sup>CAMx EGU and Onroad were identically processed as CMAQ.

<sup>c</sup>BELD v4.1 vegetation data for biogenic emissions, BEIS version is 3.61.

### 3.2 Source apportionment simulation designs

As discussed in Section 2, ISAM has been updated to include a user option with five possible configurations for source apportionment approach. Here, we conduct CMAQ source apportionment simulations for all these options: ISAM-OP1, ISAM-OP2, ISAM-OP3, ISAM-OP4 and ISAM-OP5, hereafter referred to as OP1, OP2, OP3, OP4 and OP5.

~~Additionally, the~~ [The](#) OSAT3 approach was [also](#) used in the CAMx v7.10 base model for comparison with the five ISAM simulations. Hereafter OSAT3 is referred to as OSAT. ~~For better~~

275 understanding the differences between ISAM options and OSAT used in this analysis, the source apportionment approach implemented in CAMx is briefly recapped here. ~~All available versions of OSAT (including OSAT3) in CAMx separately solve for production and destruction of O<sub>3</sub> with production being attributed to either NO<sub>x</sub> or VOC emissions, depending on which is estimated to be limiting O<sub>3</sub> production. When the ratio of PH<sub>2</sub>O<sub>2</sub>/PHNO<sub>2</sub> exceeds 0.35, the produced O<sub>3</sub> is attributed to VOC emissions, and NO<sub>x</sub> emissions below that threshold. The CAMx source apportionment implementation includes an option (OSAT-APCA) that allows for a redirection of attribution to anthropogenic emissions in situations where the limiting precursor is biogenic. That option was not used for this analysis.~~

280 In OSAT, O<sub>3</sub> attributed to NO<sub>x</sub> and VOCs is tracked as separate tracer groups. O<sub>3</sub> tracers are first adjusted to account for O<sub>3</sub> destruction processes and subsequently for net O<sub>3</sub> production, which is defined as the difference between O<sub>3</sub> production and O<sub>3</sub> destruction based on a subset of photochemical reactions that result in O<sub>3</sub> destruction. In situations where the net O<sub>3</sub> production is negative (destruction reactions dominate), all the O<sub>3</sub> tracers are proportionally decreased. When net O<sub>3</sub> production is positive, production is assigned proportionally to the sources of those emissions (NO<sub>x</sub> and VOC precursor tracers) at the time and place where O<sub>3</sub> was made. OSAT includes a group of tracers that track odd-oxygen that is consumed when O<sub>3</sub> reacts with NO to form NO<sub>2</sub> that can quickly photolyze and reform O<sub>3</sub> through a reaction with oxygen. In this situation, the O<sub>3</sub> removed from the O<sub>3</sub> tracers due to the NO + O<sub>3</sub> reaction is moved to the odd-oxygen tracers (which have separate NO<sub>x</sub> and VOC tracer groups). When NO<sub>2</sub> is photolyzed and O<sub>3</sub> formed a proportional amount of O<sub>3</sub> is taken from the odd-oxygen tracers and moved to the O<sub>3</sub> tracers.

290 Finally, a brute force method (zeroing out the entire emission stream for tracked sources in CMAQ, hereafter referred to as CMAQ-BF) was also used to compare with the ISAM options and OSAT. Eleven different emission source categories were tracked using each apportionment technique. The source categories comprise four point-source categories including electricity generating units (EGU), non-electricity generating units (NONEGU), fires (FIRE), and commercial marine vessels (CMV), and six area-source categories including on-road mobile (ONROAD), non-road mobile  
300 (NONROAD), biogenic (BIO), railway (RAIL), airports (AIRP), and other (AREA). Additionally,

OILGAS was tracked as a mixed category (both point and area) of emissions from the oil and natural gas industry in the domain. Total emissions from the above sectors have been displayed in Table 3. Finally, three predefined tracers for lateral boundary conditions (BCON), initial conditions (ICON), and other sources (OTHR) were also tracked for O<sub>3</sub> and its precursors. OTHR is used for all remaining untagged emission categories. In this study, all emissions sectors were tracked as previously mentioned above for OSAT and ISAM. For CMAQ-BF, a unique CMAQ simulation for each emission source category listed above was performed by fully removing the category's entire emission stream. CMAQ-BF apportionment was then calculated by subtracting the resulting pollutant fields from a base model simulation. However, for ICON and BCON, each was reduced by 50%, and the output field difference with the base model was scaled up by a factor of 2 to avoid numerical issues associated with very low model ICON and BCON values. As for OTHR, there is no suitable way to retain an appropriate chemical state of the troposphere after subtracting necessary emission categories, initial and boundary conditions from an original CMAQ simulation. Thus, OTHR is not being compared among CMAQ-BF, ISAM and OSAT in this study.

**Table 3. Total emissions from each sector for 4km Northeast U.S. domain (month of August 2018)**

Sector	Tons/month		Percent of Total (%)	
	NOx	VOC	NOx	VOC
AIRP	2,536	1,198	1.6	0.1
AREA	10,617	95,434	6.8	8.7
BIO	8,721	895,829	5.5	81.6
CMV	6,262	684	4.0	0.1
EGU	22,458	791	14.3	0.1
FIRE	400	5,007	0.3	0.5
NONEGU	15,020	11,323	9.6	1.0
NONROAD	23,958	33,561	15.2	3.1
OILGAS	11,053	22,526	7.0	2.1
ONROAD	49,361	30,578	31.4	2.8
RAIL	6,847	318	4.4	0.0
Total	157,233	1,097,247	100	100

**Formatted:** Font: Bold

**Formatted:** Indent: First line: 0"

### 3.3 Tracked species classes

O<sub>3</sub>, NO<sub>x</sub> and VOC species were tracked by each method. As mentioned above, ISAM tracks ~~all~~ individual oxidized nitrogen and VOC species based on selected chemical mechanism in CMAQ, whereas OSAT tracks tracer families for each. To facilitate the comparison between the two models, the ISAM species were aggregated in the same fashion as OSAT (Table 4). However, some differences still exist since species representations between the two models ~~have distinct species representation~~ are not completely the same. The nitrogen groupings NO<sub>y</sub> and RNO<sub>x</sub> (Table 4) were added to better elucidate the behavior of each model under different O<sub>3</sub> producing chemical regimes.

**Table 4. Tracked species classes between ISAM and OSAT.**

OSAT	ISAM
O <sub>3</sub>	O <sub>3</sub>
RGN=NO <sub>2</sub> +NO <sub>3</sub> +2*N <sub>2</sub> O <sub>5</sub> +INO <sub>3</sub>	<sup>1</sup> RGN=NO <sub>2</sub> +NO <sub>3</sub> +2*N <sub>2</sub> O <sub>5</sub>
NIT=NO+HONO	NIT=NO+HONO
TPN=PAN+PNA+PANX+OPAN+INTR	<sup>2</sup> TPN=PAN+PNA+PANX+INTR
NTR=NTR <sub>1</sub> +NTR <sub>2</sub> +CRON	<sup>3</sup> NTR=NTR <sub>1</sub> +NTR <sub>2</sub>
HNO <sub>3</sub>	HNO <sub>3</sub>
RNO <sub>x</sub> =RGN+NIT	RNO <sub>x</sub> =RGN+NIT
NO <sub>y</sub> =RGN+NIT+TPN+NTR+HNO <sub>3</sub>	NO <sub>y</sub> =RGN+NIT+TPN+NTR+HNO <sub>3</sub>
<sup>4</sup> VOC=1.0*PAR+1.0*MEOH+1.0*FORM+1.0*KET+2.0*ETHA+2.0*ETOH+2.0*ETH+2.0*OLE+2.0*ALD <sub>2</sub> +2.0*ALDX+2.0*ETHY+3.0*PRPA+3.0*ACET+4.0*IOLE+5.0*ISOP+6.0*BENZ+7.0*TOL+8.0*XYL+10.0*TERP	VOC=1.0*PAR+1.0*MEOH+1.0*FORM+1.0*KET+2.0*ETHA+2.0*ETOH+2.0*ETH+2.0*OLE+2.0*ALD <sub>2</sub> +2.0*ALDX+2.0*ETHY+3.0*PRPA+3.0*ACET+4.0*IOLE+5.0*ISOP+6.0*BENZ+7.0*TOL+8.0*XYL+10.0*TERP

<sup>1</sup>ISAM does not track INO<sub>3</sub>

<sup>2</sup>ISAM does not track OPAN

<sup>3</sup>ISAM does not track CRON

<sup>4</sup>OSAT VOC has been pre-calculated as equation in Table 4

### 3.4 Evaluation method and case study development

Although identical emissions and meteorological inputs are used for CAMx and CMAQ (Table 2), potential differences still exist in multiple scales and processes. Shu et al. (2017, 2022) have reported that deposition is one of the largest uncertainties between the two models when other processes are constrained. For inter-comparing ISAM and OSAT, it is not feasible to constrain all process uncertainties. Thus, we established criteria to choose representative days for ISAM and OSAT

comparisons based on the performance of their parent models rather than comparing them throughout the entire simulation period to reduce the difference that may be brought on from their parent models.

We initially set the correlation relationship ( $R^2$ ) criteria of maximum daily 8-hour averaged (MDA8) O<sub>3</sub> between CMAQ and CAMx to be above 0.7 to ensure that the performance of the two parent models is comparable. Next, ~~maximum daily 8-hour averaged (MDA8)~~ O<sub>3</sub> was also used as the indicator for case study selection since ISAM and OSAT normally are used as regulatory application with this metric. We assess the mean bias (MB) of MDA8 O<sub>3</sub> for every day to choose the days on which both models have the lowest MB for predicted MDA8 O<sub>3</sub>. Therefore, CMAQ and CAMx simulated ambient concentrations were paired in space and time with observed data from the Air Quality System (AQS, <https://www.epa.gov/aqs>) monitoring network. Hourly concentrations of total O<sub>3</sub>, NO and NO<sub>2</sub> were also compared to the AQS observations, and their bias statistical metrics were calculated as well.

## 4 Results

### 4.1 Model performance evaluation and case study selection

Figure 1 shows observed site averaged MDA8 O<sub>3</sub> and its corresponding biases predicted by CMAQ and CAMx over paired AQS sites for the entire episode. Observed site averaged MDA8 O<sub>3</sub> ranges from 30 to 50 ppbv. The performance of two models for predicting MDA8 O<sub>3</sub> varies by paired day and monitor site with the range of biases from -23 to 35 ppbv, approximately. Table S1 summarizes  $R^2$  and MB of MDA8 O<sub>3</sub> for each day for both models. Based on our criteria introduced in Section 3.4, there are 13 days on which the two models show very good correlation relationships. Among these days, two models both show good performance on predicting MDA8 O<sub>3</sub> with closest MB on Aug 09<sup>th</sup> (CMAQ/CAMx = 3.09/2.99 ppbv) and 10<sup>th</sup> (CMAQ/CAMx: 2.42/2.61 ppbv). For other days, either two models both have higher MB (> 10 ppbv), or ~~they have inconsistent predicted concentrations~~ their predictions do not agree well with each other, with a difference of MBs up to 8 ppbv. Therefore, Aug 09<sup>th</sup> and 10<sup>th</sup> were selected as a two-day case study for source apportionment comparisons. Additional evaluations of hourly O<sub>3</sub>, NO and NO<sub>2</sub> is available in Fig. S1 of the supplemental information (SI). From Fig. 2, MDA8 O<sub>3</sub> is relatively higher over east coastal urban areas with generally over 50 ppbv

but reduces to 35 ppbv at other rural areas of northeast U.S. domain. The two models predicted MDA8 O<sub>3</sub> show very good agreement spatially, underestimating MDA8 O<sub>3</sub> at sites where observed MDA8 O<sub>3</sub> is high but overestimating MDA8 O<sub>3</sub> at sites where O<sub>3</sub> is low. Similar spatial plots of hourly paired O<sub>3</sub>, NO and NO<sub>2</sub> can be found in SI (Fig S2). Table 5 and 6 respectively summarize statistical metrics for MDA8 O<sub>3</sub>, hourly O<sub>3</sub>, NO and NO<sub>2</sub> at all paired monitoring sites for the monthly O<sub>3</sub> episode and the selected two-day case study episode.

The metrics in Table 5 and 6 both show consistent results with Fig. 1 as discussed above. The changes of NO and NO<sub>2</sub> metrics are marginal from the monthly episode to the two-day case. As in Fig S1, NO and NO<sub>2</sub> concentrations are less variable than O<sub>3</sub> across days in the monthly episode, as a result, the comparison of NO and NO<sub>2</sub> are less dependent on which day is selected. Unlike NO and NO<sub>2</sub>, CAMx and CMAQ performance is statistically better in the two-day case study with lower MB for hourly O<sub>3</sub> (CMAQ/CAMx = 4.67/7.02 ppbv) and MDA8 O<sub>3</sub> (CMAQ/CAMx = 2.75/2.80) than the monthly episode (hourly O<sub>3</sub>: CMAQ/CAMx = 6.49/7.99 ppbv; MDA8 O<sub>3</sub>: CMAQ/CAMx = 5.30/4.18). The differences of MB, NMB and R<sup>2</sup> between the two models also diminish for MDA8 O<sub>3</sub> but increase for hourly O<sub>3</sub> from the monthly episode to the two-day episode. The statistical metrics of hourly O<sub>3</sub> and MDA8 O<sub>3</sub> demonstrate that the selected two-day case is suitable for a source apportionment comparison in which CAMx and CMAQ not only both have the least-biased predictions compared to observations but also show a good agreement with each other.

Formatted: Subscript

Formatted: Subscript



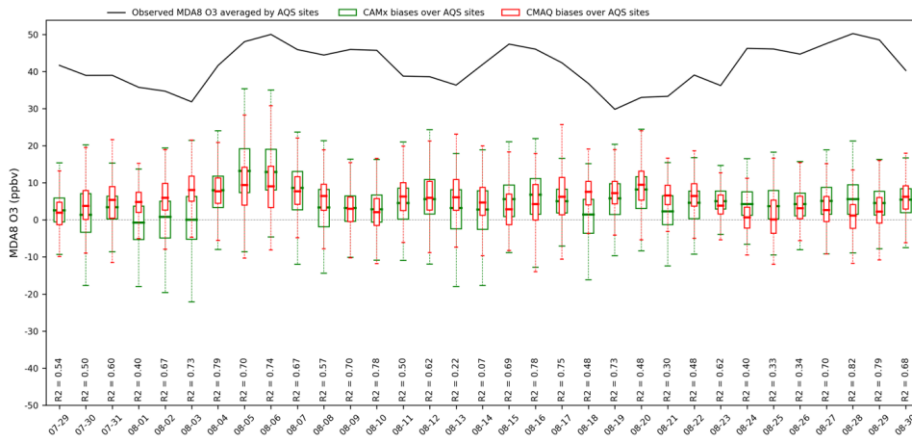


Fig.1 observed site averaged MDA8 O<sub>3</sub> and its corresponding biases predicted by CMAQ and CAMx over paired AQS sites for the entire episode. R<sup>2</sup> shows correlation relationship between CMAQ and CAMx.

385

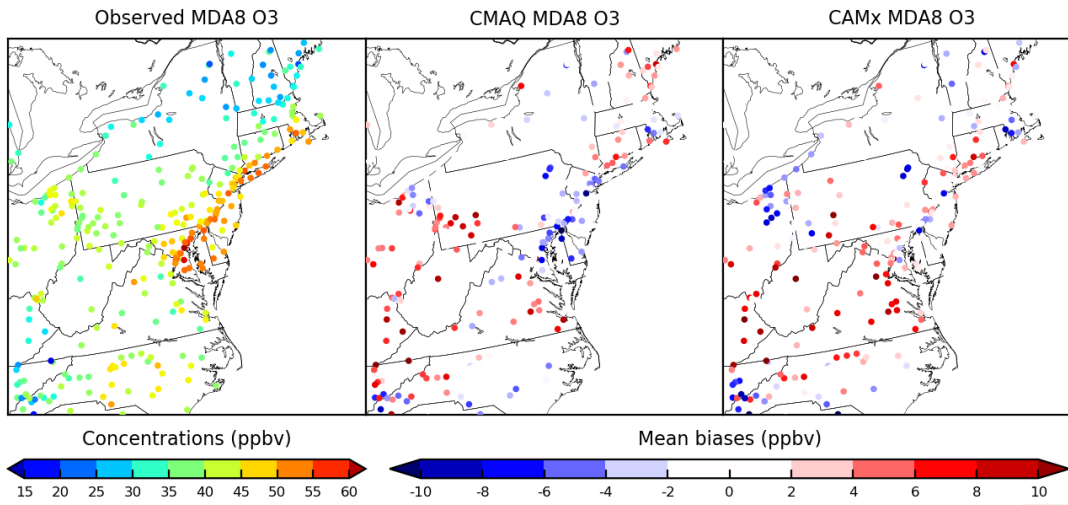


Fig.2 two-day averaged observed MDA8 O<sub>3</sub> over paired sites for northeast US domain and its corresponding mean biases predicted by CMAQ and CAMx for selected case study

**Table 5. Model performance summary at paired AQS surface monitoring sites. (Monthly episode)**

Species	Model	Number of Observations	MB <sup>a</sup>	NMB <sup>b</sup>	RMSE <sup>c</sup>	<sup>d</sup> R <sup>2</sup>
Hourly NO	CMAQ	72987	-1.05	-44.50	6.24	0.07
	CAMx	72987	-1.23	-52.25	6.39	0.05
Hourly NO <sub>2</sub>	CMAQ	61987	0.64	10.21	6.39	0.32
	CAMx	61987	1.86	29.78	7.57	0.28
Hourly O <sub>3</sub>	CMAQ	232768	6.49	23.11	11.73	0.59
	CAMx	232768	7.99	28.47	14.46	0.42
MDA8 O <sub>3</sub>	CMAQ	9409	5.30	12.80	8.23	0.64
	CAMx	9409	4.18	10.09	9.26	0.58

**Table 6. Model performance summary at paired AQS surface monitoring sites. (Two-day case study episode)**

Species	Model	Number of Observations	MB	NMB	RMSE	R <sup>2</sup>
Hourly NO	CMAQ	4264	-1.15	-48.30	6.44	0.05
	CAMx	4264	-1.38	-58.14	6.57	0.04
Hourly NO <sub>2</sub>	CMAQ	3612	0.15	2.20	6.83	0.28
	CAMx	3612	0.83	11.88	7.51	0.25
Hourly O <sub>3</sub>	CMAQ	13486	4.67	15.06	10.88	0.61
	CAMx	13486	7.02	22.65	13.26	0.49
MDA8 O <sub>3</sub>	CMAQ	567	2.75	6.00	6.28	0.62
	CAMx	567	2.80	6.10	6.95	0.63

<sup>a</sup> Mean bias:  $MB = \frac{1}{N} \sum M_i - O_i$ , MB ranges from negative infinity to positive infinity with 0 indicating unbiased data, unit here is ppbv.

<sup>b</sup> Normalized mean bias:  $NMB = \frac{1}{N} \sum \frac{M_i - O_i}{O_i}$ , ranges from negative 1 to positive infinity with 0 indicating unbiased data. The values shown in the table were multiplied by 100.

<sup>c</sup> Root mean square error:  $RMSE = \sqrt{\frac{1}{n} \sum_{i=1}^n (M_i - O_i)^2}$ , is the standard deviation of the prediction errors.

<sup>d</sup>  $R^2 = \left\{ \frac{\sum(O_i - \bar{O})(M_i - \bar{M})}{\sqrt{\sum(O_i - \bar{O})^2 \sum(M_i - \bar{M})^2}} \right\}^2$ , R<sup>2</sup> ranges from 0 to 1 with 1 indicating perfect correlation and 0 indicating an uncorrelated relationship.

## 4.2 Comparison of model source apportionment

### 4.2.1 Temporal variations of sector contributions

To better understand how the ISAM model apportionment approach simulated source contributions at each time step, time-series comparisons for each source were examined for O<sub>3</sub> and its

precursors, RNO<sub>x</sub> and VOC for the two-day case study. Figure 3 shows hourly variations of domain averaged predicted total O<sub>3</sub> (bulk) concentrations and sector contributions for seven source apportionment simulations (OSAT, BF, ISAM OP1 to OP5). In Fig. 3, CMAQ and CAMx predict similar ~~ozone~~O<sub>3</sub> concentrations during the day, but differences appear at night, with a maximum difference of 5 ppb. This disparity was discussed in Section 4.1 and can be mitigated by employing the MDA8 O<sub>3</sub> metric. The seven source apportionment simulations yield similar diurnal trends via the trajectory of the total concentrations, but they apportion concentrations to each sector somewhat differently. Comparisons of five ISAM options reveals significant variability. OP1, which apportions uniformly according to stoichiometry, shows similar trends of apportionments for each sector as OP4, an option that always allocates products to sources with reactive VOCs and their radicals. They both apportion more BCON and BIO O<sub>3</sub> but fewer contributions from all other sectors than the other three ISAM options (OP2, OP3 and OP5). Results of OP1 and OP4 would likely overestimate sensitivity to emissions to these reactants because VOCs are often available in excess. OP2 always allocates products to sources with nitrogen reactants, which prevents the attribution of NO<sub>x</sub> to non-nitrogen reactants. Typically, these non-nitrogen reactants are common in transported (e.g., BCON) or natural sources (e.g., isoprene in BIO). As a result, OP2 decreases BCON and BIO contributions while increasing contributions from other sectors relative to OP1 and OP4.

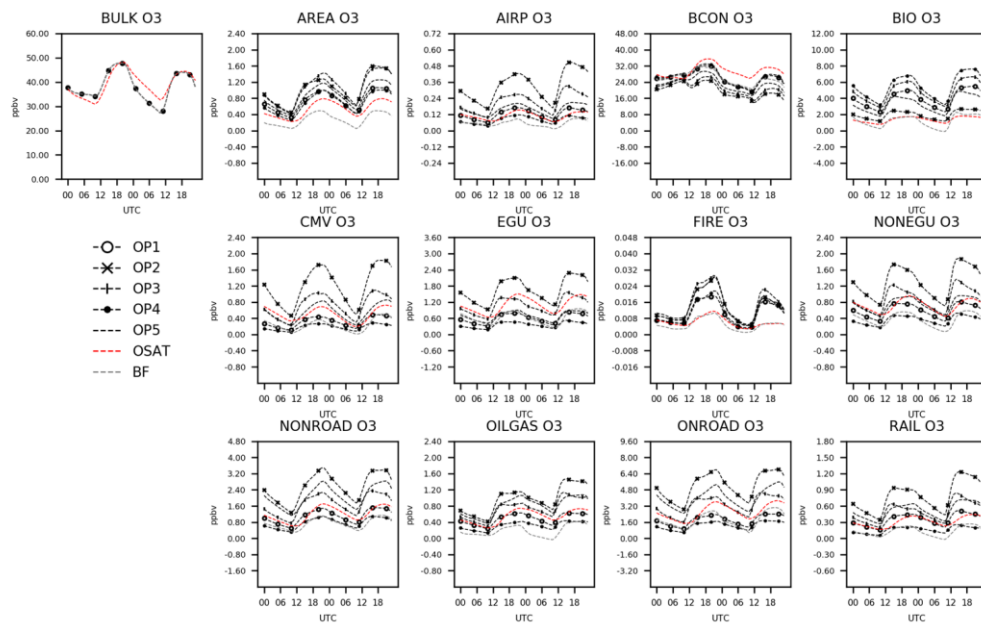
OP5 assigns products to either reactive VOCs or NO<sub>x</sub> based on the ratio of PH<sub>2</sub>O<sub>2</sub>/PHNO<sub>3</sub>, placing O<sub>3</sub> contribution results for all sectors between the previous four ISAM options. OSAT, which utilizes a similar methodology as OP5, shows consistent diurnal patterns of domain averaged total O<sub>3</sub> and sector contributions as the ISAM options, but with varying magnitudes. OSAT has the largest BCON O<sub>3</sub> but the least contributions from AREA, BIO and FIRE. The rest of the OSAT sector contributions are between the ISAM options. Consistent with earlier findings, CMAQ-BF estimates systematically smaller O<sub>3</sub> contributions for all sectors besides EGU and BCON (Kwok et al., 2015). While ISAM and OSAT appear to retain bulk mass as intended, CMAQ-BF shifts the chemical system into a different, ~~typically negative,~~ nonlinear O<sub>3</sub> response to source change.

In Fig. 4, CAMx and CMAQ predict comparable total RNO<sub>x</sub> except for the first 12 hours of the two-day example, when OSAT values deviate from those of the other six simulations. As the total

concentrations of the two models converge, OSAT exhibits similar patterns to OP2 and OP3. OP1, OP4  
435 and OP5 show comparable results, with increased BCON and BIO RNO<sub>x</sub> but decreased contributions  
from other sectors. ~~Except for BCON and BIO, CMAQ-BF results are comparable to OP2 and OSAT  
for all sectors.~~ CMAQ-BF show comparable results with OSAT, OP2 and OP3 except for BCON and  
BIO, which are negative for CMAQ-BF, suggesting that removing these source sectors results in a  
slight rise in RNO<sub>x</sub>. In previous source sensitivity and allocation investigations, it has been shown that  
440 BF may have limits when the model response contains an indirect effect coming from the influence of  
substances other than the direct precursors (Kwok et al., 2015; Burr and Zhang, 2011; Koo et al., 2009;  
Jimenez and Baldasano, 2004; Zhang et al., 2009). This would be particularly true in situations where  
emissions are a large percentage of total NO<sub>x</sub> or VOC in a particular area. The nonlinear impacts on gas  
phase chemistry realized in a source sensitivity model simulation would not be a relevant representation  
445 of culpability from that same source group.

Figure 5 illustrates the hourly variability of domain-averaged VOC concentrations and sector  
contributions. CAMx only gives pre-lumped VOC (Table 4) for OSAT outputs. For consistency, VOC  
for CMAQ ISAM and BF has also been carbon-weighted by summing all individual VOC species in  
CMAQ outputs using the same method as OSAT (Table 4). In Fig. 5, CAMx consistently simulates  
450 higher attribution to total VOC concentrations than CMAQ, with a maximum difference of 30 ppb.  
These larger CAMx VOC concentrations are also reflected in apportioned OSAT sectors, particularly  
those with substantial contributions, such as BCON and BIO. Given that the difference is present in the  
total concentration, this is unlikely caused by different source apportionment formulation between  
CMAQ and CAMx. As CAMx only gives pre-lumped VOC, it is challenging to compare individual  
455 VOC species between CMAQ and CAMx to explain this difference at current stage. Another possible  
reasons to cause it could be that models have different internal treatments for advection and diffusion,  
which can impact surface-level concentrations and indirectly impact chemical reactions. The five ISAM  
options have comparable diurnal patterns for most sectors, with the exception of CMV, EGU, and  
RAIL, however the magnitudes for these three sectors are relatively minor, which is consistent with  
460 earlier findings (Kwok et al., 2015). CMAQ-BF estimates notably lower sector contributions for VOCs,  
which is similar to O<sub>3</sub> results (Fig. 4), with negative contributions for small sectors (e.g., CMV, EGU,

and RAIL). Additional figures of other grouped nitrogen species tracked in Table 4 (e.g., RGN, HNO<sub>3</sub> and NO<sub>y</sub>) can be found in SI.



465

Fig.3 Total and attributed O<sub>3</sub> concentrations to various sectors as a function of hour of day and apportionment technique.

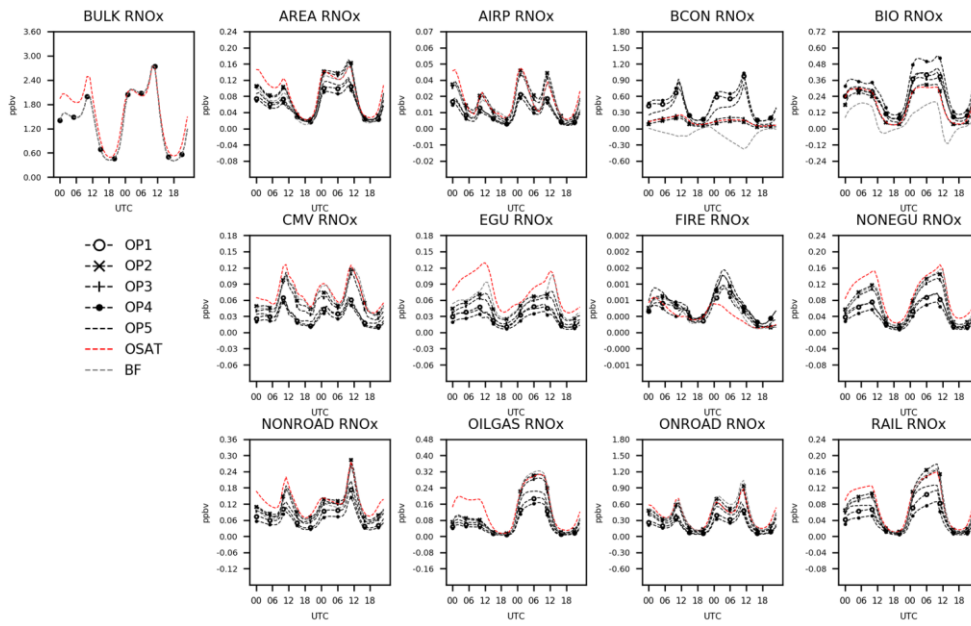


Fig. 4 Total and attributed RNO<sub>x</sub> concentrations to various sectors as a function of hour of day and apportionment technique.

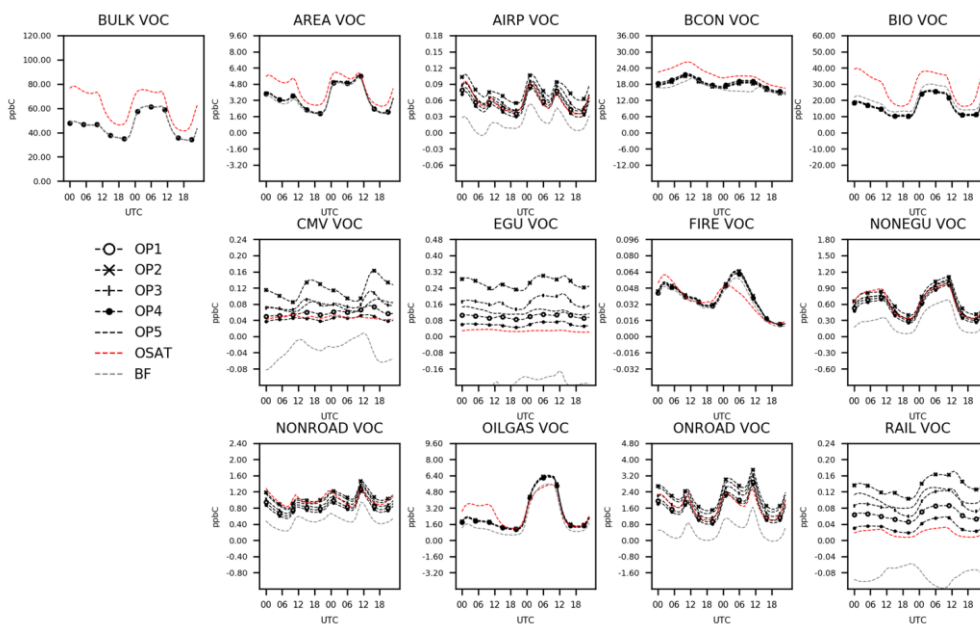


Fig. 5 Total and attributed VOC concentrations to various sectors as a function of hour of day and apportionment technique.

#### 4.2.2 Spatial distribution of source apportionment simulations

Spatial patterns of total and sector contributions of MDA8 O<sub>3</sub> (Fig. 6), RNO<sub>x</sub> (Fig. 7) and VOC (Fig. 8) have been examined for the seven simulations. In Fig. 6, OSAT exhibits the same spatial distribution of MDA8 O<sub>3</sub> total concentrations as other CMAQ-based simulations (OP1, OP2, OP3, OP4, OP5, and CMAQ-BF), with the exception of OSAT's relatively high marine and offshore total concentrations ( $\geq 5$  ppbv), which could be explained by the difference in planetary boundary layer dynamics ~~and gaseous chemical mechanism~~ or different marine chemistry configuration between the two parent models. CMAQ CB6R3 uses a rough parameterization for full marine halogen chemistry to destroy O<sub>3</sub>, depending only on land-use category and sunlight (Sarwar et al., 2015, 2019), whereas CAMx CB6R4 handles O<sub>3</sub> depletion in the marine boundary more efficiently by including the 16 most important reactions of inorganic iodine (I-16b, Emery et al., ~~2016~~2016b). According to a sensitivity test

conducted by [SmithEmery et al. \(20162016b\)](#), I-16b could reduce O<sub>3</sub> depletions by 2-5 ppbv in  
485 comparison to full halogen chemistry. Regarding sector concentrations, the spatial distributions of seven  
simulations are comparable. They can all capture geographic contribution hot spots from each sector,  
although their magnitudes vary. ~~For most sources, OSAT paradoxically shows lower contributions over  
the ocean.~~ OP2 stands out with fewer contributions from BIO than the other four ISAM options, and  
subsequently assigns larger concentrations to other sectors, particularly over east coastal regions, as  
490 shown in Fig. 3 and 6. Since OP2 assigns all products to sources with nitrogen reactants, the influence  
of reactants from biogenic sources is diminished, as intended.

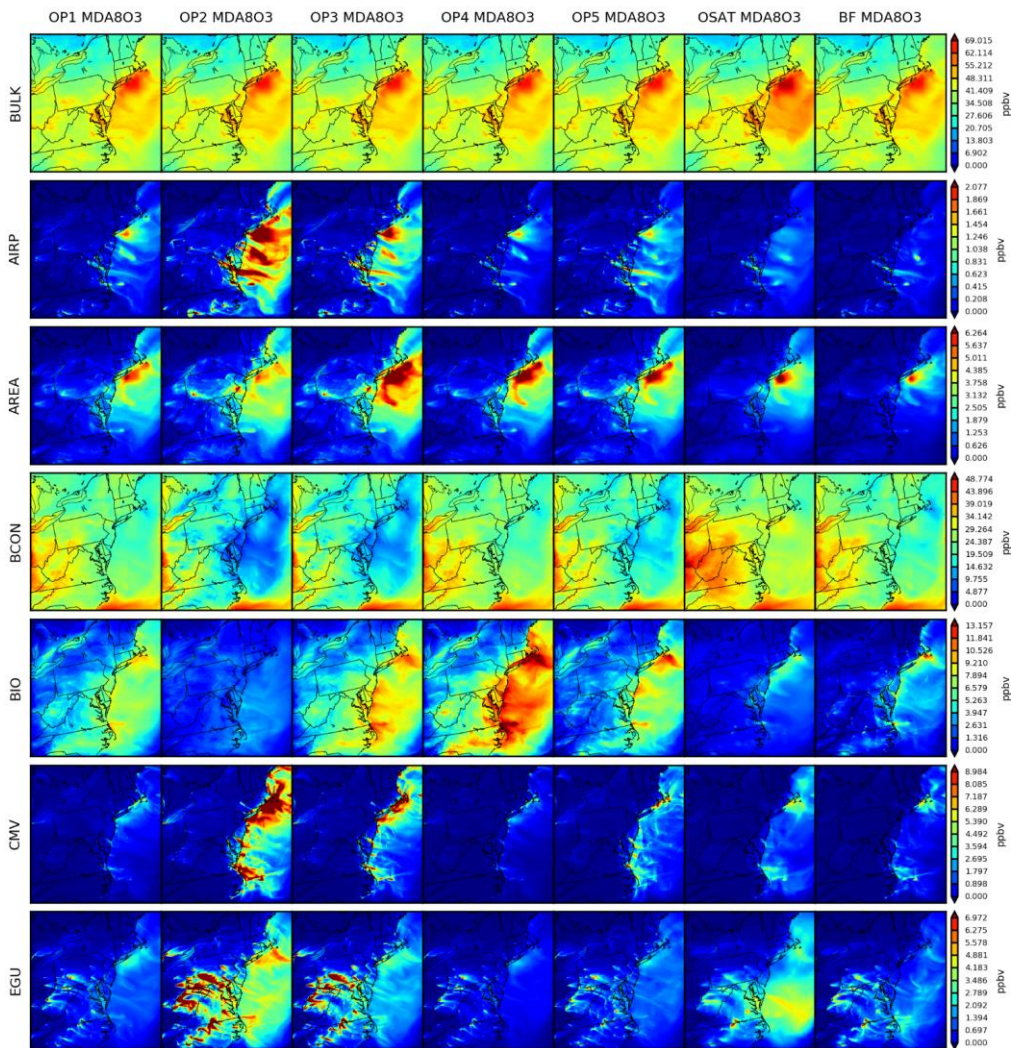
Figure 7 depicts the associated outcomes of RNO<sub>x</sub>. Except for BCON, the seven simulations  
produce geographically and quantitatively consistent findings. From the spatial distributions, we can  
conclude that local sources govern RNO<sub>x</sub> more than long-transported sources compared to O<sub>3</sub>.

495 Anthropogenic RNO<sub>x</sub> is either more concentrated in the urban areas (e.g., AREA, NONEGU,  
NONROAD), gasoline industry (OILGAS) and electric facilities (EGU) or along with transportation  
(e.g., AIRP, ONROAD, CMV and RAIL). Biogenic RNO<sub>x</sub> is more prevalent in rural locations with  
vegetation. It should be noted that OP1, OP4 and OP5 show more BCON RNO<sub>x</sub> across the entire  
domain because of the way to assign products in nitrogen related reactions (Section 2). OP1, OP4 and  
500 OP5 show local hotspots of RNO<sub>x</sub> attributed to BCON. Since there is no physical reason to suspect  
hotspots over urban areas, we conclude that these contributions represent RNO<sub>x</sub> attributed based on  
VOC or oxidants transported from the boundary. Figure 8 depicts the outcomes associated with VOC.

Higher VOC concentrations from CAMx already shown in Fig. 65 are primarily from Virginia and  
North Carolina (OSAT bulk). As CMAQ and CAMx both use the same BEIS inventory data, the  
505 difference in total VOC concentrations may result from other differences between two models, like  
chemistry or deposition, accordingly, leading to higher biogenic sources in CAMx (BIO). For the rest of  
sectors, OSAT and ISAM options are fairly consistent except that the OP2 predicts more contributions  
from EGU, CMV and RAIL. CMAQ-BF predicts consistently lower source contributions for MDA8 O<sub>3</sub>,  
RNO<sub>x</sub>, and VOC, as shown in Section 4.2.1. This yet again illustrates that brute force represents an  
510 integrated sensitivity while the OSAT and ISAM represent attribution at a point in the nonlinear  
chemical systems. Monthly averaged spatial maps for MDA8 O<sub>3</sub>, RNO<sub>x</sub>, and VOC are also included in



Fig. S4(a-c) and show consistent results as two-day averaged maps. This demonstrates that our case study is appropriate, efficiently selecting representative days as well as minimizing the uncertainties from parent models (CMAQ and CMAQ). Additional figures of other grouped nitrogen species tracked in Table 4 (e.g., RGN, HNO<sub>3</sub> and NO<sub>y</sub>) can also be found in SI.



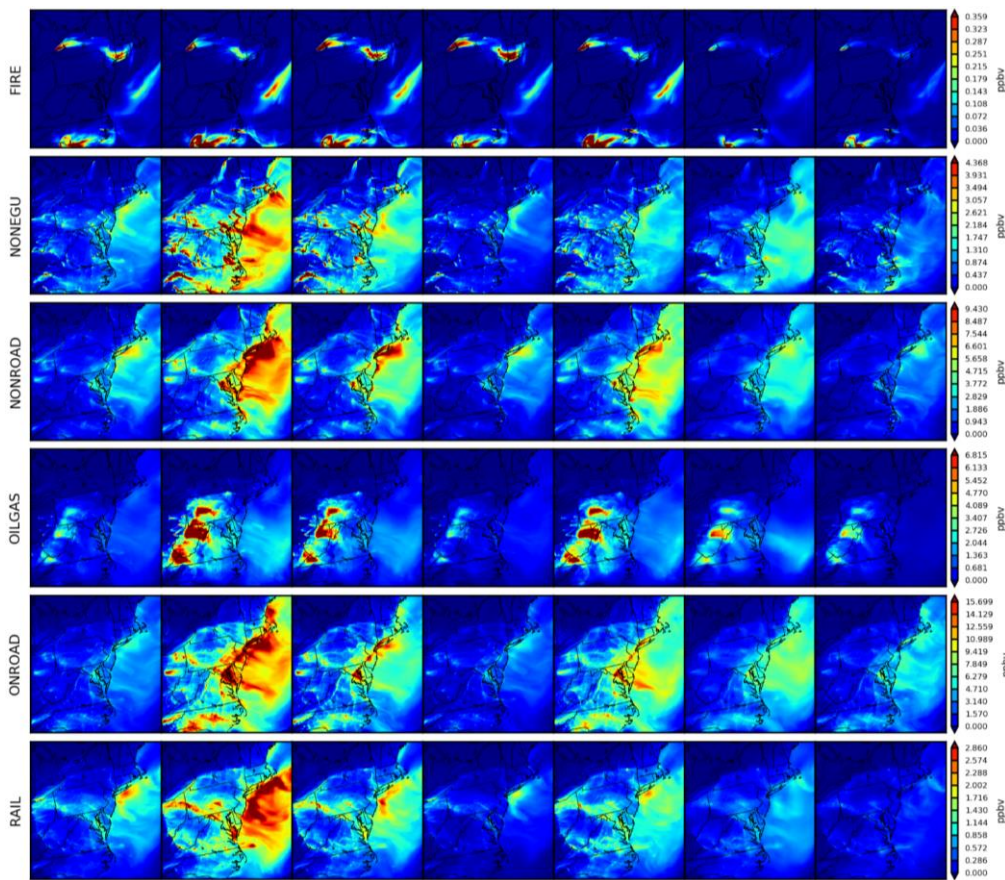
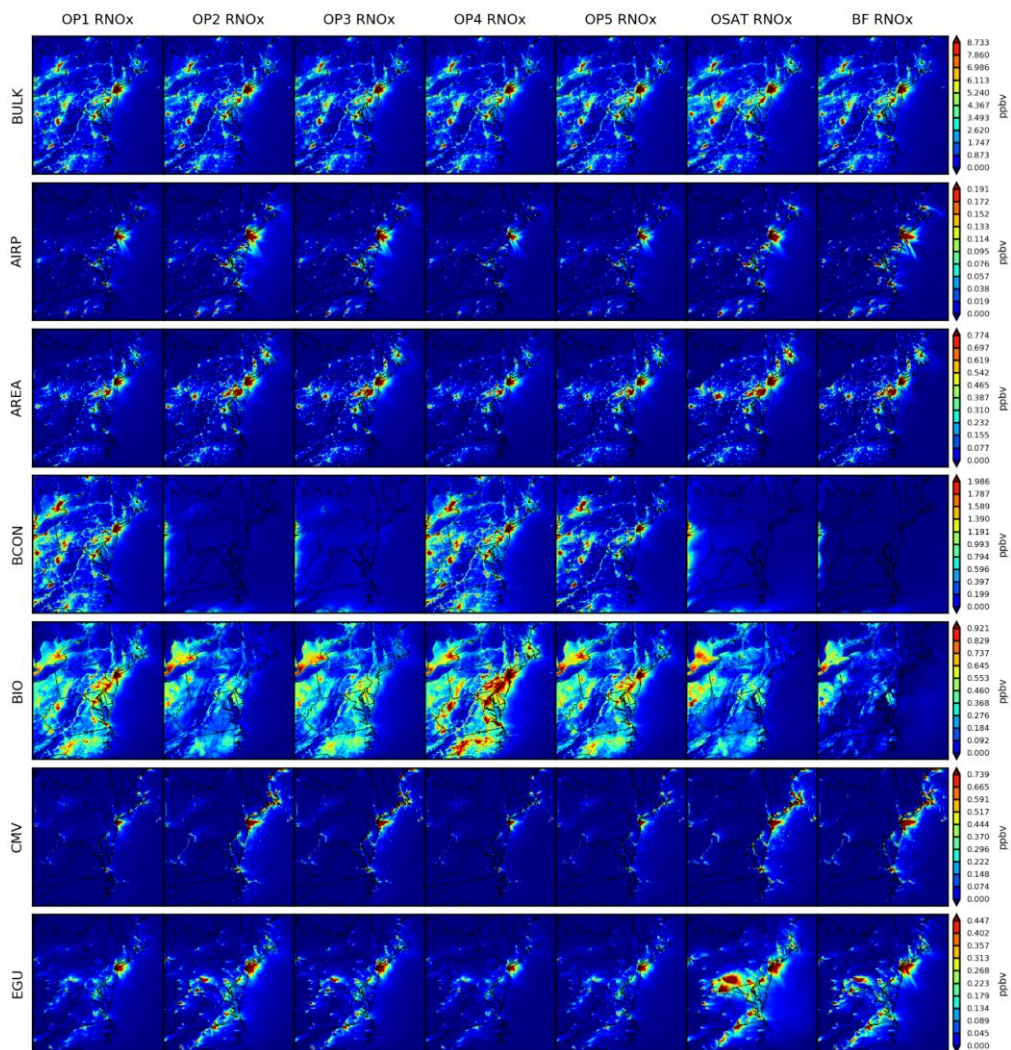


Fig. 6 Spatial comparisons of seven simulations for two-day averaged O<sub>3</sub> (08/09 and 08/10).



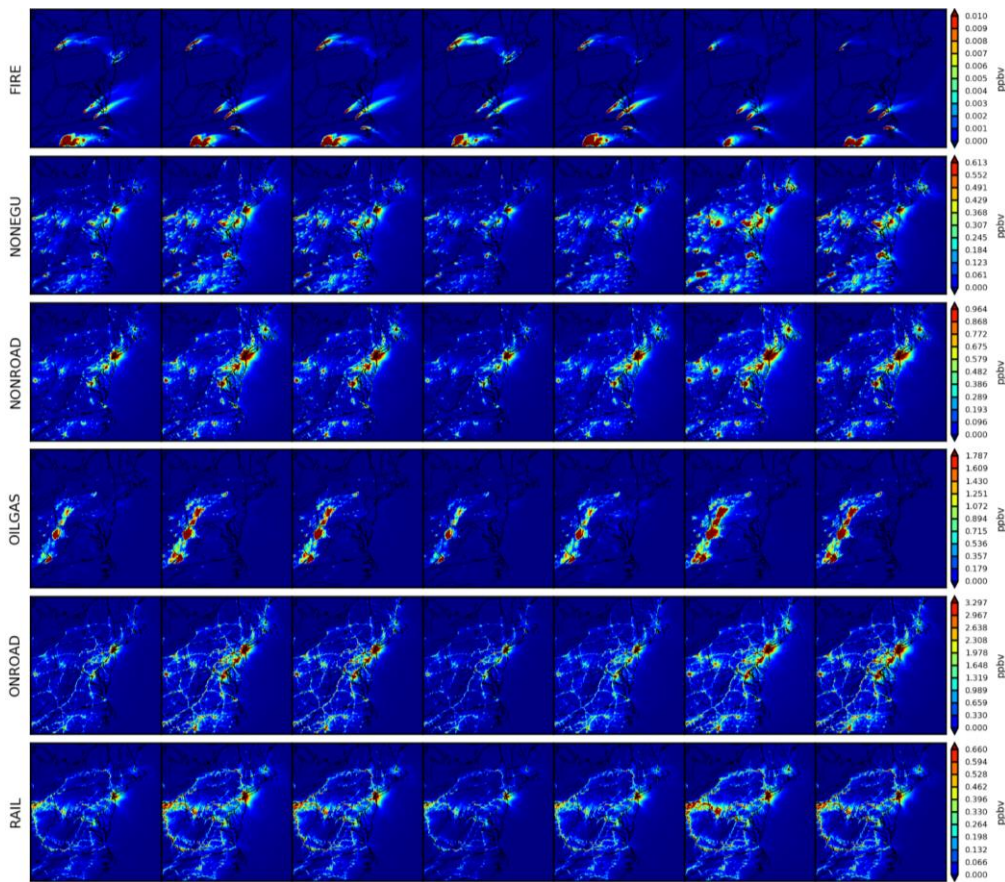
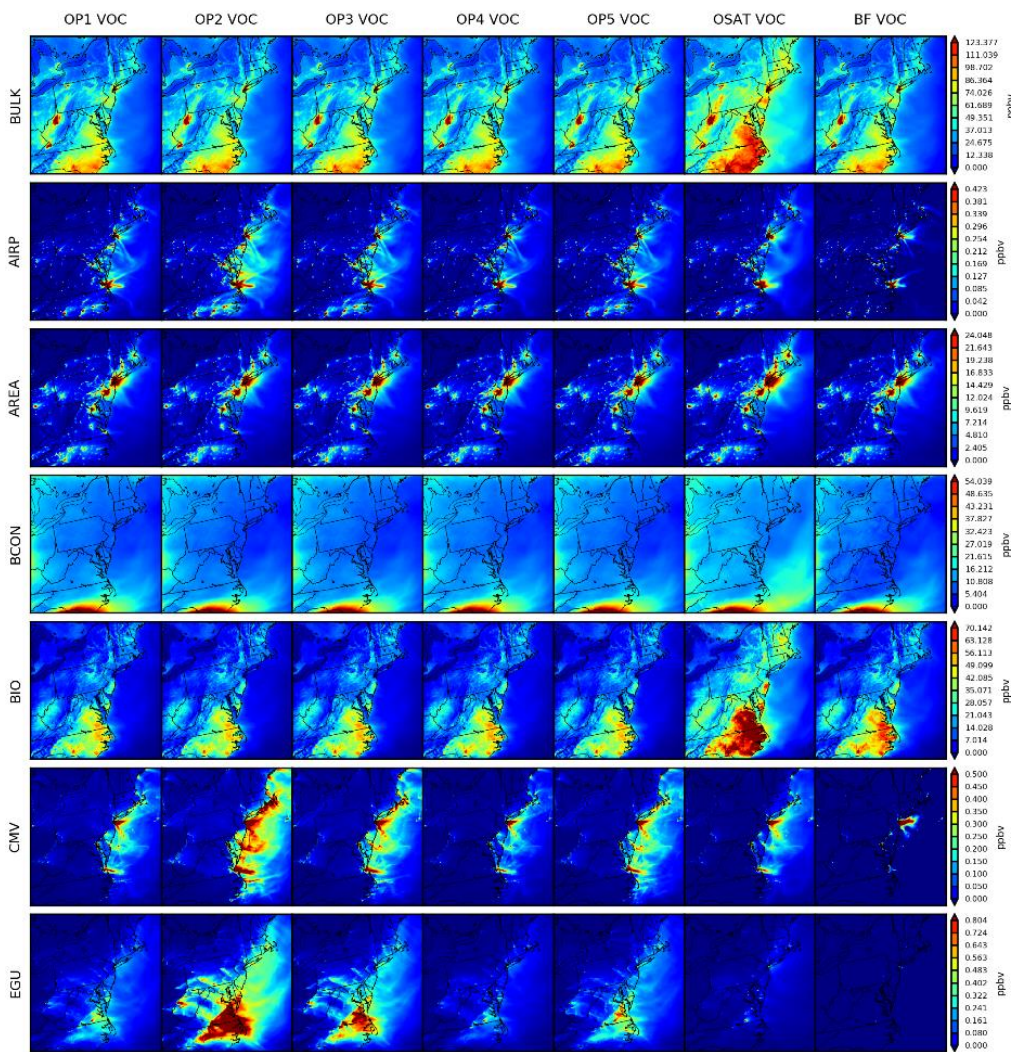


Fig. 7 Spatial comparisons of seven simulations for two-day averaged RNO<sub>x</sub> (08/09 and 08/10).



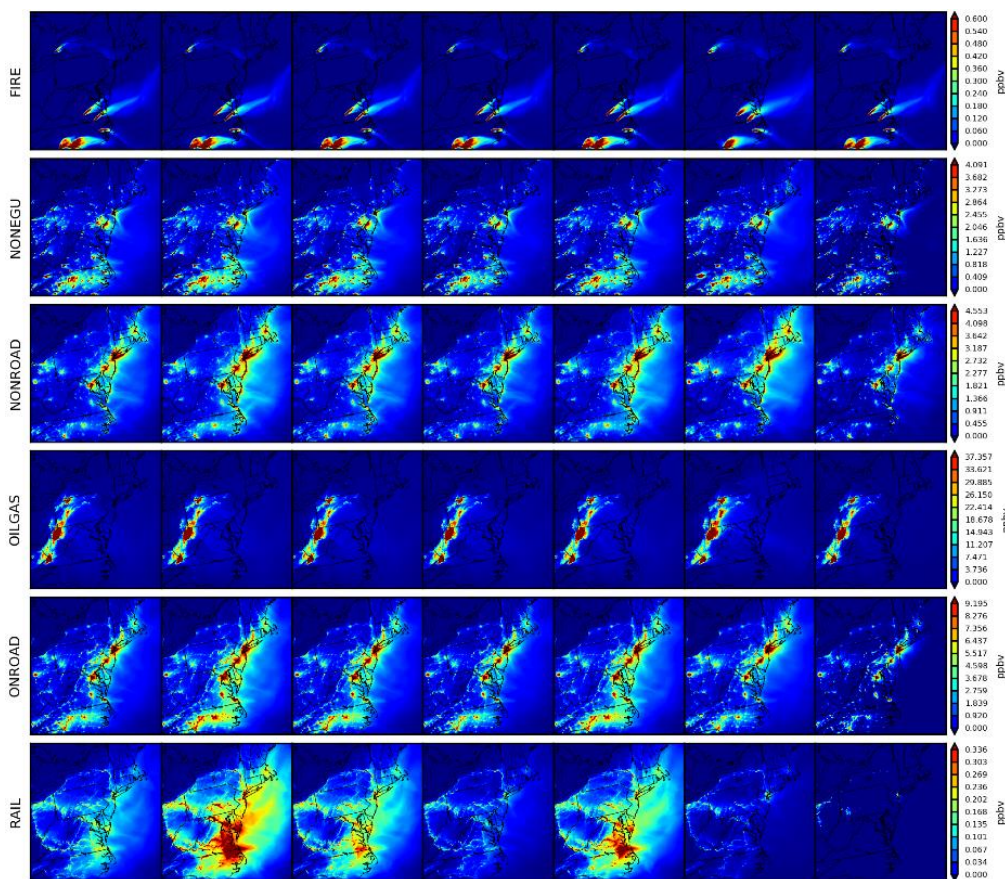


Fig. 8 Spatial comparisons of seven simulations for two-day averaged VOC (08/09 and 08/10).

## 5 Model Simulation Time

The CPU time required to complete a source apportionment simulation in a 3D AQM is an important consideration for usability. For a 4 km x 4 km simulation domain encompassing the northeast U.S., the model run times for OSAT and ISAM are similar. Using 128 processors, base CMAQ (without ISAM) and CMAQ-ISAM simulations (11 source categories) are tested. Base CMAQ requires around

60 minutes per simulation day (24 hours), whereas CMAQ-ISAM requires approximately 120 minutes. If the number of processors is increased to 256, the simulation time for CMAQ-ISAM can be reduced to 30 minutes showing good scalability. It is worth noting that our CMAQ-ISAM simulations simultaneously track all additional species classes, such as sulfate, nitrate, ammonium, elemental carbon, organic carbon, and chloride. It would shorten simulation times if related species were only tracked for O<sub>3</sub>. Base CAMx (without OSAT) and CAMx OSAT are also tested with 128 processors, taking 37 and 67 minutes, respectively. CAMx also provides an optional tool for particles that can be simultaneously applied similarly to ISAM (PSAT, Yarwood et al., 2007). When additional pollutants are selected for tracking (e.g., sulfate, primary PM<sub>2.5</sub> species, etc.) total simulation time will increase for both ISAM and OSAT/PSAT. CMAQ-BF speed is based on CMAQ base simulation (60 mins/day x (1 base + 11 sources + 1 boundary condition + 1 initial condition + 1 other) = ~~720900~~ mins/day).

## 6 Discussions and Conclusions

Source attribution approaches are generally intended to determine culpability of precursor emissions sources to ambient pollutant concentrations. Source-based apportionment approaches such as ISAM and OSAT provide similar types of information, specifically an estimate of which sources or groups of sectors (e.g., a sector) contributed to the air quality measured or estimated at a particular location. The assumptions in each technique have implications for interpretation in the context of air quality management.

Source attribution of secondarily formed pollutants cannot be explicitly measured, which makes evaluation of source apportionment approaches challenging. Here, the ISAM approach was evaluated by 1) a comparison with a source apportionment approach implemented in a different photochemical modeling system and 2) a comparison with a simple source sensitivity (brute-force difference) approach in the same modeling system that is most comparable to source apportionment in more linear systems and less useful when formation and transport is nonlinear. Further, this section notes qualitative consistency between the spatial nature of sector emission and the attribution of precursors and O<sub>3</sub> as another method to generate confidence in these approaches.



In this study, multiple apportionment approach comparisons show common features but still  
560 reveal wide variations in predicted sector contribution and species dependency. The attribution to  
sources emitting NO<sub>x</sub> and VOC is consistent with the spatial nature of these sources, which provides  
confidence in the approach. However, nitrogen species (e.g., NO<sub>x</sub>), for instance, are more sensitive to  
the choice of ISAM options than VOC. For example, although the attribution of NO<sub>x</sub> to EGUs matches  
the location of these sources (e.g., New York urban area) for all ISAM options, OP1, OP4 and OP5  
565 predict more BCON NO<sub>x</sub>. This is because the fast NO<sub>x</sub> cycling process assigns anthropogenically  
emitted nitrogen species to other sources, as the original emitted source identity is not retained through  
these complex reactions. Further, sources entirely located offshore, such as commercial marine vessels,  
do not have culpability assigned to distant inland regions of the model domain. Most of the time, the  
amount of attribution to a certain sector depends on the number of emissions from that sector, how far  
570 away those emissions are, and whether the prevailing winds carried emissions from those places to the  
monitor or grid cell where air quality was predicted.

The designed five ISAM options maximize its flexibility, particularly for modeling source  
apportionment of O<sub>3</sub> and its precursors, but the choice of option depends on target species. Among all  
ISAM options, the OP5 option, after making the assignment decision based on the ratio of PH<sub>2</sub>O<sub>2</sub> to  
575 PHNO<sub>3</sub>, is expected to predict generally similar spatial and temporal patterns for O<sub>3</sub> to the OSAT source  
apportionment approach implemented in CAMx. However, it still shows disparity for some sectors  
(e.g., biogenic sectors for O<sub>3</sub>). This result may be because of the OSAT formulation which differs from  
the ISAM options presented here. The OP5 option was also similar to brute-force sensitivity estimates  
predicted in CMAQ with the exception of source groups that dominate regional emissions or O<sub>3</sub>, such as  
580 biogenic VOC and O<sub>3</sub> introduced into the model through boundary inflow. In those situations, it is not  
reasonable to expect a source sensitivity approach to provide a useful comparison for source attribution  
given the highly nonlinear change in atmospheric chemistry. After assigning products to sources  
emitting nitrogen reactants, the OP2 option can predict results of RNO<sub>x</sub> attributions that are more  
comparable to OSAT and BF. It demonstrated that the OP2 works better for RNO<sub>x</sub> because it makes it  
585 easier to find the original source and lessens the effect of other sources when these species are cycling  
quickly through an integrated chemical reaction system. Unlike O<sub>3</sub> and RNO<sub>x</sub>, the VOC contribution for

the majority of source categories depends very little on the ISAM option. We expect that the user will use OP5 for O<sub>3</sub> and OP2 for RNO<sub>x</sub>, but this is not a firm suggestion. In turn, we give the user this flexibility so that ISAM can be used for a wide range of purposes.

590 By comparing the multiple approaches in the Northeast U.S., we found that both OSAT and ISAM attribute the majority of O<sub>3</sub> and NO<sub>x</sub> contributions to boundary, mobile, and biogenic sources, whereas the top three VOC contributions are attributed to biogenic, boundary, and area sources.

~~However, it is~~However, comparisons of OSAT and ISAM have some limits, especially when they are under the two different parent models, CAMx and CMAQ. Although we have put efforts into  
595 diminishing the differences between the two models by making most configuration options as similar as possible, some inevitable uncertainties cannot be eliminated at the current stage of this study (e.g., an imperfect match of chemical mechanisms, different internal treatments for advection, diffusion, and deposition processes). Further, it is also worthwhile to note that our results in this study are based on limited duration and specific regions, and they may not comprehensively reflect all situations. Given  
600 that the source attribution of secondary pollutants cannot be explicitly measured, these inter-comparisons between ISAM and OSAT are still useful for reference. We continue to need further efforts that combine field experiment studies and model evaluations for longer terms and multiple regions to better understand source attribution given the highly nonlinear change in nature of O<sub>3</sub>-NO<sub>x</sub> chemistry.

#### 605 **Code availability**

~~The CMAQ model documentation and released version 5.4 of the source code, including updated ISAM code used in this study, are available at [www.cmaq-model.org](http://www.cmaq-model.org). The updates described here, as well as model~~The updated ISAM code used in this study has been permanently archived at  
610 <https://doi.org/10.5281/zenodo.6266674> and has also been implemented in the newer version of CMAQ (v5.4). The CMAQ model documentation is available at <https://github.com/USEPA/CMAQ> and [www.cmaq-model.org](http://www.cmaq-model.org). Model post-processing scripts, are available upon request.

### **Data availability**

The raw observation data used are available from the sources identified in Sect. 3, while the post-processed observation data are available upon request. The CMAQ model data utilized are available  
615 upon request as well. Please contact the corresponding author to request any data related to this work.

### **Author contributions**

QS, SN, KB designed this study and experiments. QS led the development of this manuscript and was responsible for most of the model evaluation components in this study. SN, WH and BM developed the ISAM code. KB provided all the input data for the CMAQ simulations. QS carried out the CMAQ pre-  
620 processing, simulations, and post-processing, produced the figures, and prepared the initial paper draft. SN contributed directly to the writing of Sect. 2 of this paper. KB contributed directly to the writing of Sect. 6 of this paper. WH, BM, CH and BH discussed all results throughout the ISAM development and contributed to the final writing of this paper.

### **Competing interests**

625 The authors declare that they have no conflict of interests.

### **Disclaimer**

The views expressed in this article are those of the authors and do not necessarily represent the views or policies of the U.S. Environmental Protection Agency.

### **Acknowledgments**

630 This project was supported in part by an appointment to the Research Participation Program at the Office of Research and Development, US Environmental Protection Agency, administered by the Oak Ridge Institute for Science and Education through an interagency agreement between the US Department of Energy and the EPA.

## References

635 Atkinson, R.: Atmospheric chemistry of VOCs and NO<sub>x</sub>, *Atmospheric Environment*, 34, 2063–2101, [https://doi.org/10.1016/S1352-2310\(99\)00460-4](https://doi.org/10.1016/S1352-2310(99)00460-4), 2000.

~~Baker K, Timin B. PM2.5 source apportionment comparison of CMAQ and CAMX estimates. In 7th Annual Community Modeling and Analysis System (CMAS) Conference 2008 Oct 6 (pp. 6–8).~~

640 ~~Bash JO, Baker KR, Beaver MR. 2016. Evaluation of improved land use and canopy representation in BEIS v3. 61 with biogenic VOC measurements in California. *Geoscientific Model Development* 9, 2191.~~

~~Baker, K. R., M. C. Woody, G. S. Tonnesen, W. Hutzell, H. O. T. Pye, M. R. Beaver, G. Pouliot, and T. Pierce. "Contribution of regional-scale fire events to ozone and PM2.5 air quality estimated by photochemical modeling approaches." *Atmospheric Environment* 140 (2016): 539-554.~~

645 Booker, F., Muntifering, R., McGrath, M., Burkey, K., Decoteau, D., Fiscus, E., Manning, W., Krupa, S., Chappelka, A., and Grantz, D.: The Ozone Component of Global Change: Potential Effects on Agricultural and Horticultural Plant Yield, Product Quality and Interactions with Invasive Species, *Journal of Integrative Plant Biology*, 51, 337–351, <https://doi.org/10.1111/j.1744-7909.2008.00805.x>, 2009.

650 ~~Burr, Michael J., and Yang Zhang. "Source apportionment of fine particulate matter over the Eastern US Part I: source sensitivity simulations using CMAQ with the Brute Force method." *Atmospheric Pollution Research* 2, no. 3 (2011): 300-317.~~

Butler, T., Lupascu, A., Coates, J., and Zhu, S.: TOAST 1.0: Tropospheric Ozone Attribution of Sources with Tagging for CESM 1.2.2, *Geosci. Model Dev.*, 11, 2825–2840, <https://doi.org/10.5194/gmd-11-2825-2018>, 2018.

655 Cohan, D. S. and Napelenok, S. L.: Air Quality Response Modeling for Decision Support, *Atmosphere*, 2, 407–425, <https://doi.org/10.3390/atmos2030407>, 2011.

Cooper, O. R., Langford, A. O., Parrish, D. D., and Fahey, D. W.: Challenges of a lowered U.S. ozone standard, *Science*, 348, 1096–1097, <https://doi.org/10.1126/science.aaa5748>, 2015.

660 Duncan, B. N., Yoshida, Y., de Foy, B., Lamsal, L. N., Streets, D. G., Lu, Z., Pickering, K. E., and Krotkov, N. A.: The observed response of Ozone Monitoring Instrument (OMI) NO<sub>2</sub> columns to NO<sub>x</sub> emission controls on power plants in the United States: 2005–2011, *Atmospheric Environment*, 81, 102–111, <https://doi.org/10.1016/j.atmosenv.2013.08.068>, 2013.

665 Dunker, A. M., Yarwood, G., Ortmann, J. P., and Wilson, G. M.: Comparison of Source Apportionment and Source Sensitivity of Ozone in a Three-Dimensional Air Quality Model, *Environ. Sci. Technol.*, 36, 2953–2964, <https://doi.org/10.1021/es011418f>, 2002.

Emery, C., ~~J~~-Jung-~~B~~-J, Koo, ~~G~~-B., Yarwood, G. 2015. Improvements to CAMx Snow Cover Treatments and Carbon Bond Chemical Mechanism for Winter Ozone. Final report for Utah Department of Environmental Quality, Division of Air Quality, Salt Lake City, UT, August 2015, available at

670 [http://www.camx.com/files/udaq\\_snowchem\\_final\\_6aug15.pdf](http://www.camx.com/files/udaq_snowchem_final_6aug15.pdf)~~http://www.camx.com/files/udaq\_snowchem\_final\_6aug15.pdf~~ (last accessed 13 December 2019).

~~Emery, C., Z. Liu, B. Koo, G. Yarwood. 2016. Emery, C., Koo, B., Hsieh, W. C., Wetland, A., Wilson, G., Yarwood, G. 2016(a) Technical Memorandum for Updated Carbon Bond Chemical~~

675 [Mechanism. EPA Contract EPD12044, available at https://www.camx.com/files/emaq4-07\\_task7\\_techmemo\\_r1\\_laug16.pdf](https://www.camx.com/files/emaq4-07_task7_techmemo_r1_laug16.pdf) (last accessed 1 February 2023).

Emery, C., Liu, Z., Koo, B., Yarwood, G. 2016(b). Improved Halogen Chemistry for CAMx Modeling. Final report for Texas Commission on Environmental Quality WO 582-16-61842-13, May 2016, available at [https://www.tceq.texas.gov/airquality/airmod/project/pj\\_report\\_pm.html](https://www.tceq.texas.gov/airquality/airmod/project/pj_report_pm.html) (last accessed 13 December 2019).

680 [Gillani, N. V., & Pleim, J. E. \(1996\). Sub-grid-scale features of anthropogenic emissions of NO<sub>x</sub> and VOC in the context of regional Eulerian models. \*Atmospheric Environment\*, 30\(12\), 2043-2059.](#)

Grewe, V., Tsati, E., and Hoor, P.: On the attribution of contributions of atmospheric trace gases to emissions in atmospheric model applications, *Geosci. Model Dev.*, 3, 487–499, <https://doi.org/10.5194/gmd-3-487-2010>, 2010.

685 [Henderson, B. H., F. Akhtar, H. O. T. Pye, S. L. Napelenok, and W. T. Hutzell. "A database and tool for boundary conditions for regional air quality modeling: description and evaluation." \*Geoscientific Model Development\* 7, no. 1 \(2014\): 339-360.](#)

Hidy, G. M., Friedlander, S. K.: "The Nature of the Los Angeles Aerosol," p 391 in "Proceedings of the Second International Clean Air Congress" Academic Press, London, 1971.

Jacob, D. J. and Winner, D. A.: Effect of climate change on air quality, *Atmospheric Environment*, 43, 51–63, <https://doi.org/10.1016/j.atmosenv.2008.09.051>, 2009.

Jacquemin, B. and Noilhan, J.: Sensitivity study and validation of a land surface parameterization using the HAPEX-MOBILHY data set, *Boundary-Layer Meteorol*, 52, 93–134, <https://doi.org/10.1007/BF00123180>, 1990.

695 [Jiménez, P., Pedro, and José M. Baldasano. "Ozone response to precursor controls in very complex terrains: Use of photochemical indicators to assess O<sub>3</sub>-NO<sub>x</sub>-O<sub>3</sub>-NO<sub>x</sub>-VOC sensitivity in the northeastern Iberian Peninsula." \*J. Geophys. Res.\*, " \*Journal of Geophysical Research: Atmospheres\* 109, D20309, <https://doi.org/10.1029/2004JD004985>, no. D20 \(2004\).](#)

700 [Karamchandani, P., Long, Y., Pirovano, G., Balzarini, A., and Yarwood, G.: Source-sector contributions to European ozone and fine PM in 2010 using AQMEII modeling data, \*Atmos. Chem. Phys.\*, 17, 5643–5664, <https://doi.org/10.5194/acp-17-5643-2017>, 2017.](#)

Koo, B., Wilson, G. M., Morris, R. E., Dunker, A. M., and Yarwood, G.: Comparison of Source Apportionment and Sensitivity Analysis in a Particulate Matter Air Quality Model, *Environ. Sci. Technol.*, 43, 6669–6675, <https://doi.org/10.1021/es9008129>, 2009.

705 [Kwok, R.-H.-F., Baker, K.-R., Napelenok, S.-L., and Tonnesen, G.-S., 2015. Photochemical grid model implementation and application of VOC, NO<sub>x</sub> and O<sub>3</sub> source apportionment. \*Geosci. Geoscientific Model Development\*, 8, \(1\), pp.99–114, <https://doi.org/10.5194/gmd-8-99-2015>.](#)

710 [Kwok, R. H. F., Napelenok, S. L., and Baker, K. R.: Implementation and evaluation of PM<sub>2.5</sub> source contribution analysis in a photochemical model, \*Atmospheric Environment\*, 80, 398–407, <https://doi.org/10.1016/j.atmosenv.2013.08.017>, 2013.](#)

Lamsal, L. N., Duncan, B. N., Yoshida, Y., Krotkov, N. A., Pickering, K. E., Streets, D. G., and Lu, Z.: U.S. NO<sub>2</sub> trends (2005–2013): EPA Air Quality System (AQS) data versus improved observations from the Ozone Monitoring Instrument (OMI), *Atmospheric Environment*, 110, 130–143, <https://doi.org/10.1016/j.atmosenv.2015.03.055>, 2015.

715

Lefohn A. S., Leighton, P.A.: Photochemistry of Air Pollution, Academic, San Diego, California, 1961.

Shadwick D. S. and Ziman S. D., 1998. The Difficult Challenge of Attaining EPA's New Ozone Standard. Environmental Science & Technology. 32(11):276A-282A.

Li, Y., Ying, A.K.-H., Lau, A.K.-J.C.-H., Fung, J. C. H., Y. Zheng, L. J. Y., Zhong, L. J., and Peter Kwok Keung Louie, P.-K.-K., "Ozone source apportionment (OSAT) to differentiate local regional and super-regional source contributions in the Pearl River Delta region, China: OZONE SOURCE APPORTIONMENT STUDY, J. Geophys. Res., " Journal of Geophysical Research: Atmospheres 117, n/a n/a, <https://doi.org/10.1029/2011JD017340>, no. D15 (2012-).

Marmur, A., Unal, A., Mulholland, J. A., and Russell, A. G.: Optimization-Based Source Apportionment of PM<sub>2.5</sub> Incorporating Gas-to-Particle Ratios, Environ. Sci. Technol., 39, 3245–3254, <https://doi.org/10.1021/es0490121>, 2005.

Olmans, S. J., Lefohn, A. S., Scheel, H. E., Harris, J. M., Levy, H., Galbally, I. E., Brunke, E. G., Meyer, C. P., Lathrop, J. A., Johnson, B. J., Shadwick, D. S., Cuevas, E., Schmidlin, F. J., Tarasick, D. W., Claude, H., Kerr, J. B., Uchino, O., and Mohnen, V.: Trends of ozone in the troposphere, Geophys. Res. Lett., 25, 139–142, <https://doi.org/10.1029/97GL03505>, 1998.

Paatero, Pentti, and Unto Tapper. "Positive matrix factorization: A non-negative factor model with optimal utilization of error estimates of data values." Environmetrics 5.2 (1994): 111-126.

Pay, M. T., Gangoiti, G., Guevara, M., Napelenok, S., Querol, X., Jorba, O., and Pérez García-Pando, C.: Ozone source apportionment during peak summer events over southwestern Europe, Atmos. Chem. Phys., 19, 5467–5494, <https://doi.org/10.5194/acp-19-5467-2019>, 2019.

Ramboll Environ. Final Report "Improved OSAT, APCA and PSAT Algorithms for CAMx". Contract. 2015 Aug; 582:15-50417.

Ramboll Environ. Final Report "Implementation of the Piecewise Parabolic Method for Vertical Advection in Comprehensive Air Quality Model with Extensions (CAMx)". Contract. 2022 June; 582-19-90500.

Reitze Jr AW. Air Quality Protection Using State Implementation Plans-Thirty-Seven Years of Increasing Complexity. Vill. Envtl. LJ. 2004; 15:209.

Sarwar, G., Fahey, K., Napelenok, S., Roselle, S., and Mathur, R.: Examining the impact of CMAQ model updates on 1095 aerosol sulfate predictions, The 10th Annual CMAS Models 3 User's Conference, October, Chapel Hill, NC, 2011.

Sarwar, G., Gantt, B., Foley, K., Fahey, K., Spero, T. L., Kang, D., Mathur, R., Foroutan, H., Xing, J., Sherwen, T., and Saiz-Lopez, A.: Influence of bromine and iodine chemistry on annual, seasonal, diurnal, and background ozone: CMAQ simulations over the Northern Hemisphere, Atmospheric Environment, 213, 395–404, <https://doi.org/10.1016/j.atmosenv.2019.06.020>, 2019.

Sarwar, G., Gantt, B., Schwede, D., Foley, K., Mathur, R., and Saiz-Lopez, A.: Impact of Enhanced Ozone Deposition and Halogen Chemistry on Tropospheric Ozone over the Northern Hemisphere, Environ. Sci. Technol., 49, 9203–9211, <https://doi.org/10.1021/acs.est.5b01657>, 2015.

Shu, L., Wang, T., Han, H., Xie, M., Chen, P., Li, M., and Wu, H.: Summertime ozone pollution in the Yangtze River Delta of eastern China during 2013–2017: Synoptic impacts and source

apportionment, *Environmental Pollution*, 257, 113631, <https://doi.org/10.1016/j.envpol.2019.113631>, 2020.

760 Shu, Q., Koo, B., Yarwood, G., and Henderson, B. H.: Strong influence of deposition and vertical mixing on secondary organic aerosol concentrations in CMAQ and CAMx, *Atmospheric Environment*, 171, 317–329, <https://doi.org/10.1016/j.atmosenv.2017.10.035>, 2017.

Shu, Q., Murphy, B., Schwede, D., Henderson, B. H., Pye, H. O., Appel, K. W., ... & Perlinger, J. A. (2022). Improving the particle dry deposition scheme in the CMAQ photochemical modeling system. *Atmospheric Environment*, 289, 119343.

765 [Sillman, Sanford. "The use of NO<sub>y</sub>, H<sub>2</sub>O<sub>2</sub>, and HNO<sub>3</sub> as indicators for ozone-NO<sub>x</sub>-hydrocarbon sensitivity in urban locations." \*Journal of Geophysical Research: Atmospheres\* 100, no. D7 \(1995\): 14175-14188.](#)

Simon, H., Reff, A., Wells, B., Xing, J., and Frank, N.: Ozone Trends Across the United States over a Period of Decreasing NO<sub>x</sub> and VOC Emissions, *Environ. Sci. Technol.*, 49, 186–195, <https://doi.org/10.1021/es504514z>, 2015.

770 Skamarock, W., Klemp, J., Dudhia, J., Gill, D., Barker, D., Wang, W., Huang, X.-Y., and Duda, M.: A Description of the Advanced Research WRF Version 3, UCAR/NCAR, <https://doi.org/10.5065/D68S4MVH>, 2008.

775 [Smith J, Emery C, Liu Z, Koo B, Yarwood G. Final Report Improved Halogen Chemistry for CAMx Modeling. Contract. 2016 May; 582:15-50417.](#)

[Stein, U. and Alpert, P.: Factor Separation in Numerical Simulations, \*J. Atmos. Sci.\*, 50, 2107–2115, \[https://doi.org/10.1175/1520-0469\\(1993\\)050<2107:FSINS>2.0.CO;2\]\(https://doi.org/10.1175/1520-0469\(1993\)050<2107:FSINS>2.0.CO;2\), 1993.](#)

780 [Smith, W.P., Nicholls, M.E. and Pielke Sr, R.A., 2020. The role of radiation in accelerating tropical cyclogenesis in idealized simulations. \*Journal of the Atmospheric Sciences\*, 77\(4\), pp.1261-1277.](#)

T. Pierce and L. Bender, Examining the Temporal Variability of Ammonia and Nitric Oxide Emissions from Agricultural Processes Proceedings of the Air and Waste Management Association/U.S. Environmental Protection Agency Emission Inventory Conference, Raleigh October 26-28, 1999, Raleigh NC.

785 [USU.S. EPA Office Of Research And Development:\(2019\). CMAQ ISAM, Zenodo, <https://doi.org/10.5281/ZENODO.6266674>, 2022zenodo.3585898.](#)

[US EPA Office Of Research And Development: CMAQ, Zenodo, <https://doi.org/10.5281/ZENODO.5213949>, 2021.](#)

790 [US EPA, 2021. <https://www.epa.gov/air-emissions-modeling/2016-version-1-technical-support-document>](#)

[U.S. EPA \(2021\). <https://www.epa.gov/air-emissions-modeling/2016-version-1-technical-support-document>](#)

[U.S. EPA \(2022a\). CMAQ Zenodo. <https://doi.org/10.5281/zenodo.7218076>.](#)

795 [U.S. EPA \(2022b\). CMAQ Zenodo. <https://doi.org/10.5281/zenodo.6266674>.](#)

Valverde, V., Pay, M. T., and Baldasano, J. M.: Ozone attributed to Madrid and Barcelona on-road transport emissions: Characterization of plume dynamics over the Iberian Peninsula, *Science of The Total Environment*, 543, 670–682, <https://doi.org/10.1016/j.scitotenv.2015.11.070>, 2016.

World Health Organization. Global tuberculosis report 2013. World Health Organization; 2013.

Formatted: Normal, Indent: First line: 0.5"

- 800           Watson, John G., John A. Cooper, and James J. Huntzicker. "The effective variance weighting  
for least squares calculations applied to the mass balance receptor model." *Atmospheric Environment*  
(1967) 18.7 (1984): 1347-1355.
- Yarwood G, Morris RE, Wilson GM. Particulate matter source apportionment technology  
(PSAT) in the CAMx photochemical grid model. In *Air Pollution Modeling and Its Application XVII*  
805 2007 (pp. 478-492). Springer, Boston, MA.
- Yienger, J. J. and Levy, H.: Empirical model of global soil-biogenic NO<sub>x</sub> emissions, *J.*  
*Geophys. Res.*, 100, 11447, <https://doi.org/10.1029/95JD00370>, 1995.
- Zhang, L., Jacob, D. J., Kopacz, M., Henze, D. K., Singh, K., and Jaffe, D. A.: Intercontinental  
source attribution of ozone pollution at western U.S. sites using an adjoint method, *Geophys. Res. Lett.*,  
810 36, L11810, <https://doi.org/10.1029/2009GL037950>, 2009.
- Zhang, R., Cohan, A., Pour Biazar, A., and Cohan, D. S.: Source apportionment of biogenic  
contributions to ozone formation over the United States, *Atmospheric Environment*, 164, 8–19,  
<https://doi.org/10.1016/j.atmosenv.2017.05.044>, 2017.